A Feasibility Study of Using The AFRODITE Clover Detectors As Compton Polarimeters

Nceba Mhlahlo

A thesis submitted in partial fulfilment of the requirements
for the degree of Master of Science
in the Department of Physics
University of Cape Town

July 2000

A Feasibility Study Of Using The AFRODITE Clover Detectors As Compton Polarimeters

Abstract

A technique used to measure the linear polarisation of γ-rays has been described and demonstrated using the AFRODITE (African Omnipurpose Detector For Innovative Techniques and Experiments) Clover detectors at the National Accelerator Centre (NAC), located in Faure near Cape Town. The feasibility study of measuring the linear polarisation of γ-rays using the AFRODITE spectrometer at the NAC has been done for the first time and the sensitivity of the Clover detectors to linear polarisation has been measured by internal calibration of the polarimeter, using γ-rays of known polarisation. The polarisation sensitivity, Q, of the Clover detector has been measured and found to be 0.34 ± 0.06 at 339.0 keV and 0.24 ± 0.02 at 635 keV.

The application of the polarimeter and its performance has been investigated on ^{165}Ta nuclei. The multipolarities of ^{165}Ta γ-lines have been determined. The polarimeter has been used as an aid in building and confirming the energy level scheme of ^{165}Ta.

Acknowledgements

To:

- my supervisor, Dr R. Fearick[α], for his support and supervision throughout the duration of this project,
- Dr R. T. Newman[β], for his help and assistance with the software at NAC and for his guidance
- Prof. Sharpey-Shafer[β], for his advice and for special lectures he gave me on the subject of polarisation
- Prof. P. Butler[φ], for answering some of my questions on polarisation and for sending me computer programs on this subject
- Prof. D. G. Aschman[α] and
- Dr E. Gueorguieva[β], for their help in checking and in making corrections on the drafts of my thesis
- Dr Kobus Lawrie[β], for availing himself to answer some of my question on polarisation and on some computer programming

[0]α: University of Cape Town, β: National Accelerator Centre, φ: University of Liverpool, Liverpool, U.K.

- David Roux, for providing me with the ^{164}Hf and ^{165}Ta data for analysis

- my family (my mother and my sister, Loni), for their patience and support

- my friends, colleagues, brothers and sisters (Pheello, Rodney, Nthabiseng, Mphuthi, Matoto, Thembani and others), for being good and kind to me,

  and last but certainly not least to my friend, God, for giving me strength to carry on,

  I would like to express my sincere appreciation and gratitude

Nceba Mhlahlo, *Cape Town, July 2000*

Contents

List of Figures

List of Tables

Chapter 1

INTRODUCTION

Linear polarisation is a measure of the orientation of the electric field of the detected γ-rays. In order to measure the polarisation, a system consisting of nuclei with spins preferentially oriented along a certain axis or plane is needed.

For a radio-active source like ^{152}Eu, the spins of the nuclei are isotropically oriented in space with the magnetic substates, m, equally populated. Such a system is said to be unoriented. In a heavy-ion in-beam reaction, residual nuclei have more spins oriented on the plane normal to the beam direction. Such a system is polarised and this polarisation can be measured. Polarisation measurements are useful in resolving ambiguities associated with the construction of decay level schemes of nuclei. By determining the multipole order (dipole or quadrupole) and the nature of radiation (electric or magnetic), assisted by multipole selection rules for gamma decay, spins and parities of nuclear states can

be assigned and level schemes be constructed.

In general, there are four techniques used to measure the polarisation of γ-rays: the photodisintegration of the deuteron used to detect linear polarisation by means of nuclear emulsions soaked in D_2O, the Compton magnetic polarimeter for detecting circular polarisation by transmission, the Compton magnetic polarimeter for detecting circular polarisation by forward scattering and the Compton polarimeter which is used for detecting linear polarisation [Fag59].

The Compton polarimeter technique has been used in this work to measure the linear polarisation of γ-rays. This has been achieved by making use of the sensitivity of Clover detectors to polarisation due to high probability of Compton scattering of γ-rays between adjacent elements of a composite detector. By combining this information with angular distribution measurements, the spins and parities of nuclear states can be determined by in-beam γ-measurements.

In this work I report on

i) the use of the AFRODITE (African Omnipurpose Detector For Innovative Techniques and Experiments) Clover detector array to construct and measure the anisotropy and the sign of linear polarisation of ^{164}Hf γ-rays using data acquired for the

^{142}Nd(^{27}Al, $4np$) reaction at a beam energy, E, of 150 MeV.

ii) the internal calibration of detectors at 90° with respect to the beam axis for their sensitivity to linear polarisation using selected ^{164}Hf γ-rays (210.8 keV, 339.0 keV, 376.4 keV, 498.2 keV, 566.9 keV, 583.7 keV and 635.6 keV) of well known $E2$ transitions.

iii) the application of the polarimeter to investigate the linear polarisation of γ-rays associated with decay of high spin states in ^{165}Ta nuclei and the subsequent determination of their sign of polarisation, the radiation character, and the multipolarity for high spin studies.

iv) how part of a level scheme of ^{165}Ta constructed at NAC (National Accelerator Centre) by the time this report was written, has been confirmed and how $E2$ and $M1$ transitions have been identified using the polarisation measurements done at NAC.

Chapter 2

THEORETICAL BACKGROUND

2.1 THE γ-RAY POLARISATION FORMALISM

2.1.1 Introduction

The linear polarisation is a measure of the direction of the electric field, **E**, of the detected γ-rays. The Compton scattering process provides a way of measuring this polarisation. The standard definition of γ-ray linear polarisation, $P(\eta)$, is given by

$$P(\eta) = \frac{J_0(\eta, \xi = 0°) - J_{90}(\eta, \xi = 90°)}{J_0(\eta, \xi = 0°) + J_{90}(\eta, \xi = 90°)} \qquad (2.1)$$

where $J_0(\eta, \xi)$ is the intensity of the polarised radiation with its electric vector making an angle $\xi = 0°$ with the reaction plane (the plane containing the incident particle beam) and $J_{90}(\eta, \xi)$ is the intensity of the polarised radiation with its electric vector making an angle $\xi = 90°$ with the reaction plane. The angle η gives the direction of the detector relative to the beam direction. Equation 2.1 is derived and discussed in [Fag59].

As it can be seen in equation 2.1 above, linear polarisation can be measured by taking the difference between the intensities of radiations with an electric vector parallel to the reaction plane ($\xi = 0°$) and those with an electric vector perpendicular to that plane ($\xi = 90°$), with $P(\eta)$ normalized to the total intensity of radiation. One can also measure $P(\eta = 90°)$ by determining the experimental values of the angular distribution coefficients. Angular distributions are discussed in detail below.

2.1.2 Angular Distributions

The angular distribution function is defined as

$$W(\eta) = \frac{I_\gamma(\eta)}{I_\gamma(\text{tot})} = 1 + a_2 P_2(\cos\eta) + a_4 P_4(\cos\eta) \quad (2.2)$$

where

$$P_2(\cos\eta) = \frac{1}{2}(3\cos^2\eta - 1) \tag{2.3}$$

and

$$P_4(\cos\eta) = \frac{1}{8}(35\cos^4\eta - 30\cos^2\eta + 3) \tag{2.4}$$

$I_\gamma(\eta)$ is the intensity of radiation at angle η and $I_{\gamma(\mathrm{tot})}$ is the total intensity for normalisation [Gue99].

The values of the angular distribution coefficients, a_2 and a_4 used to determine the linear polarisation of γ-rays, can be obtained by fitting the measured γ-ray intensities at each angle, $I_\gamma(\eta)$, using equation 2.2. Angular distributions can be analysed using known quadrupole transitions. The signs of the angular distribution coefficients determine the multipole order of radiation. For a pure stretched ($\Delta I = 1$, where I is the angular momentum) dipole, the intensity of γ-rays at 90° is greater than that at 45° and 135°, and the value of a_2 is negative while $a_4 = 0$.

For a stretched ($\Delta I = 2$) quadrupole, the intensity of γ-rays at 90° is less than that at 45° and 135°, and the value of a_2 is positive and that of a_4 is very small.

We have checked if the determined coefficients, a_2 and a_4, are consistent with the multipolarity (dipole or quadrupole) of the transition being studied [Gue99]. Caution has also been taken when measurements of coefficients were done as both stretched

($\Delta I = 2$) and non-stretched ($\Delta I = 0$) transitions give a positive value of a_2 [Gue99]. Linear polarisation measurements help solve this problem as they give more information about the multipolarity of transitions.

Once the angular distribution coefficients are extracted from equation 2.2, the expression

$$P_\gamma(\theta = 90°) = \pm\frac{3a_2 + 1.25a_4}{2 - a_2 + 0.75a_4} \tag{2.5}$$

is used to calculate the degree of polarisation, P_γ, for pure dipole or quadrupole transitions [Slt94]. Since the polarisation effect is maximum at 90° for quadrupole radiation, only detectors at this angle are considered for analysis.

The full formalism describing the angular distributions and linear polarisation of γ-rays can be found in [Fag59].

2.2 THE KLEIN-NISHINA FORMULA

A Compton polarimeter makes use of the dependence and sensitivity of the Compton scattering process to linear polarisation. This dependence and sensitivity can be obtained from the Klein-Nishina formula which gives the differential cross-section for the process.

2.2.1 The Compton Scattering Cross-Section

The probability of Compton scattering of incident γ-rays through an angle θ depends upon the angle between the scattering plane containing θ and the plane normal to the electric vector, **E**, of the radiation.

The differential form of the Klein-Nishina formula gives the differential cross-section of the Compton scattering process and shows how this process is dependent on the linear polarisation of γ-rays. The differential cross-section for Compton scattering is defined as

$$\frac{d\sigma}{d\Omega} = \frac{r_0^2}{2}\frac{E^2}{E_i^2}\left[\frac{E}{E_i} + \frac{E_i}{E} - 2\sin^2\theta\cos^2\varphi\right] \tag{2.6}$$

where

$$r_0 = e^2 m_0 c^2 \tag{2.7}$$

is the classical radius of the electron, $d\Omega$ is the element of the solid angle into which the γ-ray is scattered, θ is the angle through which the incident γ-ray is scattered, φ is the angle between the electric vector of the incident γ-ray and the plane of scattering. E_i and E are the energies of the incident and scattered photons, respectively. Equation 2.6 is obtained after

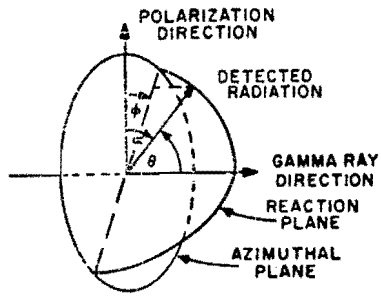

Figure 2.1: *Angles and vectors involved in a reaction sensitive to the linear polarisation of a γ-ray.*

summing over all directions of the electric vector of the scattered radiation [Fag59]. The energies, E_i and E, in equation 2.6 are related by the kinematic equation of Compton scattering:

$$E = \frac{E_i}{1 + (E_i/m_0c^2)(1 - \cos\theta)} \tag{2.8}$$

The angles and vectors involved in a Compton scattering process are shown in Figure 2.1. Figure and caption have been obtained directly from [Fag59]. A modified version of Figure 2.1 can be found in [Slt94].

Equation 2.6 shows that scattering is prefered in the plane normal to the electric vector of the incident photon, i.e. the differential cross-section, $d\sigma/d\Omega$, is maximum at $\varphi = 90°$ [Sch98]. At low energies, equation 2.6 predicts that the asymmetry be-

tween γ-rays scattered vertically and those scattered horizontally in a detector should be maximum for $\theta = 90°$ [Fag59]. By taking the difference between a spectrum of γ-rays scattered vertically and those scattered horizontally in a detector, this anisotropy can be constructed and measured and can be used to measure the linear polarisation of γ-rays.

2.2.2 Gamma-ray Anisotropy

For a Clover detector, where events can scatter horizontally and vertically between any two adjacent elements of the detector, the following expression for experimental scattering anisotropy is used

$$A(\eta) = \frac{N_{\perp} - N_{||}}{N_{\perp} + N_{||}} \tag{2.9}$$

where $N_{||}$ is the number of coincident counts in the reaction plane (the plane defining the beam direction) and $N_{\perp}$ is the number of coincident counts perpendicular to that plane [Wer95].
$N_{\perp}$ and $N_{||}$ in equation 2.9 for experimental anisotropy above can be expressed in terms of equation 2.6 as

$$N_{\perp} = J_0(\eta, \xi = 0°)\frac{d\sigma}{d\Omega}(\theta, \varphi = 90°) + J_{90}(\eta, \xi = 90°)\frac{d\sigma}{d\Omega}(\theta, \varphi = 0°) \tag{2.10}$$

and

$$N_{\|} = J_0(\eta, \xi = 0°)\frac{d\sigma}{d\Omega}(\theta, \varphi = 0°) + J_{90}(\eta, \xi = 90°)\frac{d\sigma}{d\Omega}(\theta, \varphi = 90°) \tag{2.11}$$

where $J(\eta, \xi)$ is the intensity of the polarised γ-ray emitted in the direction of an angle η with respect to the beam direction with their polarisation vector in a plane at an angle ξ to the reaction plane.

It can be seen from equations 2.6 and 2.10 that at low energies and when $\theta = 90°$ and $\varphi = 90°$, $N_{\perp}$ is maximum. This is expected since the differential cross-section is maximum at $\varphi = 90°$ and minimum at $\varphi = 0°$. This will only happen when the electric vector of the incident photon is parallel to the beam direction ($\eta = 0°$). Scattering of the incident photon will be favoured only in the direction normal to the beam axis. The same can be said about $N_{\|}$ in equation 2.11. Under similar conditions, if the electric vector of the incident photon is normal to the beam direction then the photon will be scattered in a vertical direction parallel to the beam axis. By measuring the difference between $N_{\perp}$ and $N_{\|}$ the linear polarisationof the γ-rays and the character of the radiation can be determined.

2.3 COMPTON POLARIMETERS

2.3.1 An Ideal Polarimeter

Linear polarisation can be measured using a device known as a Compton polarimeter. Various types of Compton polarimeters have been developed in various laboratories to measure the linear polarisation of γ-rays [Sch98, Bro69, Jon95].

Linear polarisation is a measure of the direction of the electric field of a γ-ray, and Compton polarimeters provide a means and serve as an efficient tool to measure it. In general, a polarimeter that uses the Compton effect consists of a scatterer and an absorber which detects the scattered γ-rays.

The ideal polarimeter would consist of five point-like detectors [Sch98]: one central scatterer and four surrounding detectors of scattered radiation, with all detectors lying in a plane perpendicular to the incident γ-ray and with the azimuthal angle between the detectors of scattered radiation being 90°. The performance, basic design and merits of the five-point detector system are discussed in [Wer95].

The polarisation sensitivity of the ideal polarimeter is discussed in Section 2.4 below.

2.3.2 HPGe Detectors As Polarimeters

HPGe (high purity germanium) detectors used to measure the linear polarisation of γ-rays have good energy resolution for detection of γ-rays, when compared to NaI polarimeters [Bro69], ranging from $\leq$ 1 keV at 122 keV to about 2 keV at 1332 keV [Bea96] and have been used in our experiment to test their viability as Compton polarimeters.

First generation Compton polarimeters which were operative in the early 1950s consisted of scatterers made of aluminium with a Geiger counter used to detect the scattered γ-rays [Fag59, Bro69]. These devices were used to study linear polarisation of annihilation radiation emitted by a radioactive source [Met50]. Second generation polarimeters consisted of organic scintillators, one acting as a scatterer and the other as a detector of scattered radiation [Fag59, Bro69]. These were used due to their low Z. An organic scintillator makes a good scatterer since it allows radiation to scatter freely from its atoms.

The scintillators were later replaced with NaI(Tl) which gave higher efficiency and better energy resolution for the detection of γ-rays. Measurements were later made with Ge(Li) detectors which were found to give better energy resolution than NaI detectors [Twi72, Bro69]. Today HPGe (high purity germanium)

crystals are widely used in multidetector arrays as composite detectors with even better energy resolution compared to polarimeters mentioned above [Wer95, Jon95, Bea96].

As interest in measuring the linear polarisation of γ-rays increased, different types of polarimeters were designed, each representing different combinations of detector materials, coincidence efficiency, polarisation sensitivity, energy resolution, technical construction and cost. The most widely used Compton polarimeters have relatively high efficiency and can be categorised into conventional, planar and composite Compton polarimeters [Twi72, Bea96, Bas79]. These polarimeters are described in more detail below.

2.3.3 Conventional Compton Polarimeters

The conventional method for measuring the linear polarisation of γ-rays is to use a γ-ray polarimeter consisting of two or more NaI(Tl) and Ge(Li) detectors [Twi72]. One is used as a scatterer and defines the direction of the incident γ-ray and the direction in which it is Compton scattered, and the other serves as an absorber in which the scattered radiation is detected at different angles relative to the scatterer.

The performance of the two- and three-crystal systems to mea-

sure the linear polarisation has been investigated [Bro69, But72] and their sensitivity to linear polarisation was measured.

2.3.4 Planar Compton Polarimeters

A planar detector consists of a single Ge(Li) or NaI(Tl) crystal that can be rotated by 90° intervals about a vertical axis in order to record spectra at different positions. An example of a planar detector is found in [Twi72] where a Ge(Li) detector of dimensions 35 x 15 x 6 mm was used as a polarimeter. Most planar polarimeters are segmented into a number of elements, ranging from two to sixteen [Urb87]. Each segment can serve as a scatterer or an absorber of radiation.

A quantitative comparison has been made between conventional and planar polarimeters using the figure-of-merit, $Q^2\varepsilon$, (a figure that is normaly quoted when comparing polarimeters' performance). $Q = P/A$ is the polarisation sensitivity of the detector and ε is the coincidence efficiency defined as

$$\varepsilon_{coinc} = \frac{N_{\perp} + N_{\parallel}}{N_s} \tag{2.12}$$

where N_s is the total number of singles events (events totally absorbed by one element or segment of the detector) incident on the detector and $N_{\perp}$ and $N_{\parallel}$ are the number of counts scattered

in the vertical and horizontal planes of the detector respectively. At low energies, single planar detectors have a low value of Q (a factor of four less) compared to conventional polarimeters [Twi72].

The general performance of the planar detector and its characteristics were studied and it was found to be poor compared to conventional polarimeters [Twi72], [Tar68].

Since Q depends on the diameter of a crystal it is believed that increasing the volume of planar detectors can improve the value of Q for these detectors and thus making them competitive at low energies. Also, their detection efficiency can be improved although at the expense of their energy resolution.

2.3.5 Composite Detectors

When the characteristics of the two and three Ge(Li) crystal (conventional polarimeters) and planar polarimeters are studied, it is found that the Ge(Li) Compton polarimeter is much more efficient and sensitive to polarisation than the latter as discussed in Section 2.3.4 [Twi72, Lju72].

However, to achieve even higher photopeak efficiencies and polarisation sensitivity, the volume of the crystals has to be increased, resulting in the deterioration of their energy resolution

due to Doppler broadening which is maximum at 90°. A large number of detectors is thus needed for achieving a higher total photopeak efficiency without degrading the energy resolution of the detectors and increasing the collection time of electron-hole pairs produced in a crystal.

A number of detector arrays with composite detectors have been developed with increased relative and photopeak effeciencies to look into this question [Bea96, Lie95].

First generation detector arrays consisted of large single-crystal Ge detectors closely packed together. An example of such an array is the TESSA3 array, which used to be situated at the Daresbury Laboratory in the United Kingdom and had a total photopeak efficiency of 0.5% at 1332 keV. This array was used in the discovery of the first superdeformed(SD) rotational band in the ^{152}Dy nucleus in 1986 [Twi86, Duc99].

The advent of second generation γ-ray spectrometers such as GASP, EUROGAM-I and GAMMASPHERE, having up to 239 individual hyperpure Ge detectors, saw the photopeak efficiency increased up to 6% at 1332 keV [Bea96]. However, problems related to Doppler broadening of the γ-lines at 90° due to the large volume of the crystals and the subsequent deterioration in energy resolution and poor resolving power (spectrum quality),

forced reseachers to develop new types of Ge detectors.

Detector arrays consisting of composite detectors like the Clover (four HPGe crystals in a common cryostat) and the Cluster (seven HPGe crystals) detectors were developed to address some of these problems [Bea96, Lie95].

The clover detector which is used in EUROGAM-II, AFRODITE and in other arrays is the first composite detector to be used in a large array of γ-ray spectrometers.

The EUROBALL Cluster detector has also been used recently as a Compton polarimeter despite its unusual geometry [Her99]. Since the individual crystals of a Clover minimise the effect of Doppler broadening at 90° due to their small size (50 mm in diameter and 70 mm long before shaping), a large detector can be created which has a very high photopeak efficiency (10% for EUROGAM-II and about 6% for AFRODITE) and a high resolving power. One of the most important advantages of the clover detector is its sensitivity to linear polarisation due to the high probability of a γ-ray incident on one crystal Compton scattering into an adjacent element of the same detector at 90°, as predicted by the Klein-Nishina formula.

In a composite detector, signals from each crystal are summed together. Also, signals resulting from scattering between any

two or more adjacent elements of the detector are summed to give full energy signals. Using this information, an experimental anisotropy can be determined and linear polarisation be measured.

2.4 Polarisation Sensitivity

The degree of linear polarisation is related to the anisotropy of γ-rays by

$$A(\eta) = Q(E_\gamma)P(\eta) \tag{2.13}$$

where $Q(E_\gamma)$ is the polarisation sensitivity of the detector [Sch98]. The sensitivity, Q, of a Compton polarimeter may be expressed using equations 2.1, 2.13, 2.9, 2.10 and 2.11 above as

$$Q(\theta, E_\gamma) = \frac{\frac{d\sigma}{d\Omega}(\theta, \varphi = 90°) - \frac{d\sigma}{d\Omega}(\theta, \varphi = 0°)}{\frac{d\sigma}{d\Omega}(\theta, \varphi = 90°) + \frac{d\sigma}{d\Omega}(\theta, \varphi = 0°)} \tag{2.14}$$

and can be measured.

Solving equation 2.6 at $\varphi = 0°$ and at $90°$ and substituting for $\frac{d\sigma}{d\Omega}$ in 2.14 we get,

$$Q(E_\gamma) = \frac{\sin^2\theta}{\frac{E}{E_i} + \frac{E_i}{E} - \sin^2\theta} \tag{2.15}$$

which is an equation for the analysing power of the Compton scattering [Slt94], [Wer95]. [Slt94] shows plots of the analysing power of the Compton scattering against scattering angle. The plots may be useful when one wants to do Compton scattering experiments or measurements as they give the angles and energies where Compton scattering is optimal.

At $\theta = 90°$, equation 2.15 becomes

$$Q_0(\theta = 90°, E_\gamma) = \frac{1}{\frac{E}{E_i} + \frac{E_i}{E} - 1} \tag{2.16}$$

which is the equation of polarisation sensitivity for the setup of point-like detectors.

By constructing an experimental anisotropy, A, using equation 2.13 and relating it with $P(\eta)$, the polarisation sensitivity of a detector, $Q(E_\gamma)$, (a positive number between zero and one) can be determined.

Substituting for

$$\frac{E}{E_i} = \frac{m_e c^2}{m_e c^2 - E_i} \tag{2.17}$$

from the Compton kinematic equation

$$E = \frac{E_i}{1 + \frac{Ei}{m_e c^2}(1 - \cos\theta)} \tag{2.18}$$

at $\theta = 90°$ in equation 2.16 we get

$$Q_0(E_\gamma) = \left(\frac{1}{E_i/m_e c^2 + m_e c^2/(E_i + m_e c^2)}\right) \tag{2.19}$$

which is an expression for polarisation sensitivity equation for an ideal polarimeter. Equation 2.19 can also be expressed as

$$Q_0(E_\gamma) = \frac{1+\alpha}{1+\alpha+\alpha^2} \tag{2.20}$$

where

$$\alpha = E_\gamma/m_0^2 \tag{2.21}$$

is the photon energy in units of the electron rest energy [Wer95]. Equation 2.19 can be used for most Compton polarimeters including the Clover detector since it gives fairly good approximation to their energy dependence [Jon95]. In most cases, the measured values of Q are fitted using a function:

$$Q(E_\gamma) = Q_0(E_\gamma)(XE_\gamma + Y) \tag{2.22}$$

where X and Y can be obtained from a linear least-squares fit. In [Jon95] it is shown that the polarisation sensitivity for a Clover is reduced by about 71% compared to point-like detectors. This is due to the Clover geometry; its individual crystals are closely packed together.

Chapter 3

AFRODITE CLOVER DETECTORS AS POLARIMETERS

3.1 INTRODUCTION

The experiment used for polarisation measurements analysed in this work was performed using the AFRODITE spectrometer at the NAC in 1998. Excited states of, among others, ^{164,165}Ta, were populated in the ^{142}Nd(^{27}Al, xn) reactions at the beam energy of 150 MeV. The target thickness was 750 μg/cm^2. The analysis of four weekends of data acquired from the experiment was done off-line.

3.2 THE AFRODITE DETECTOR ARRAY

The AFRODITE (African Omnipurpose Detector For Innovative Techniques and Experiments) array is a spectrometer that is used at NAC to study nuclear structure at high spins. The array consists of eight Clovers and seven LEPS (Low Energy Photon Spectrometer) detectors. The detectors are arranged in rings of 45°, 90° and 135° around a target chamber where a target is placed before an experiment. The effect of Doppler broadening which is maximum at 90° is reduced for these detectors, resulting in reduced degration in energy resolution. Furthermore, their sensitivity to the linear polarisation of the incident radiation is a great advantage as it enables a clear determination of the multipolarity of γ-rays.

Figure 3.1 shows the AFRODITE array-frame, rhombicuboctahedral in shape, with 18 facets to accommodate the detectors. The figure has been taken from [NAC98]. The beam-line is also shown. Pictures of the AFRODITE array are shown in Appendix B. The figures-of-merits of the array are discussed in detail in [NAC98].

3.2.1 The AFRODITE Clover Detectors

An AFRODITE Clover detector consists of four separate coaxial HPGe (high purity germanium) crystals or elements, closely packed together and housed in a common cryostat. Figure 3.2.1 shows a schematic arrangement of a Clover. The dimensions and other properties of the Clover detector are shown in Figure 3.2.1 and in Table 3.2.1. Figure 3.2.1 is taken from [Gue99] and Table 3.2.1 and its caption from [NAC98].

Each Clover element has its own associated preamplifier and can act as a scatterer or an absorber of radiation. A photon totally absorbed in one element of the detector gives the total energy of the incident γ-ray. This is called the 'singles' event and occurs when only one element of a Clover registers a pulse height above threshold. If a signal from one element is measured in coincidence with that from another element from the same event, due to the Compton scattering of a γ-ray between the two elements, then the resulting pulse-heights are summed to give the total energy of the incident γ-ray. This is termed 'add-back'. Add-back is a result of Compton scattering of a γ-ray between adjacent elements of a detector.

Events where a cross-scattering between any two adjacent elements of the detector occurs provide information on the direc-

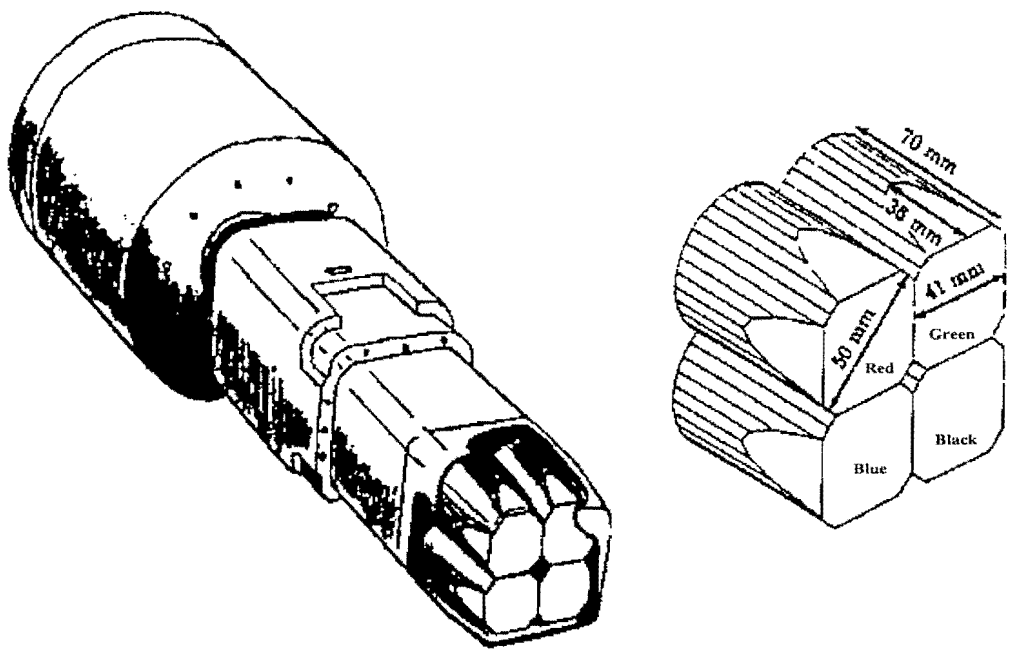

Figure 3.2.1: *A view of the Clover detector (left) consisting of four Ge crystals housed in a common cryostat and the details of the HPGe-crystal (right). A BGO suppression shield is shown mounted behind the detector.*

tion of scattering. Photons can be scattered either vertically ($N_{\perp}$) or horizontally ($N_{\parallel}$) in the detector with respect to the beam direction depending on the direction of the electric vector of the incident γ-ray.

The add-back process forms a very important basis of this work as it will allow us to determine the polarisation and the multipolarities of the γ-ray transitions using the AFRODITE Clover detectors and further provide information on parity change between the initial and final nuclear states.

3.2.2 Electronic Configuration

Figure 3.2 shows a block diagram of the electronic arrangement used during the in-beam and out-of-beam experiments. The output pulses from the detector pre-amplifiers were shaped and amplified using CAEN 16 channel N568 amplifiers. The CAEN amplifier output consists of analogue and logic pulses. The former of these are fed to 4418/V Silena ADC (Analog-to-Digital Converters) for recording the pulse heights, whereas the later provide logic information via a CFD (Constant Fraction Discriminator).

Bits labelling detector hits were set by hardware via the N415 CFD (Constant Fraction Discriminator) and the 4418/V Silena

SPECIFICATION	DETECTOR	
	Clovers	Compton suppressors
Supplier	Eurisys Mesures	Crismatec
Number at the NAC	8	8
CRYSTAL:		
Type	HPGe	BGO
Length	70 mm	26 cm
Diameter	50 mm[x]	-
Thickness	-	(4-20) mm
L_{ec}	20 mm	-
L_{tc}	194.5 mm	-
total opening angle[y]	23.2°	-
solid angle per detector[z]	1.35	-

Table 3.2.1: *Technical specifications of the AFRODITE spectrometer.* L_{ec} *and* L_{tc} *denote the distance from detector end-cap to crystal surface and the distance from the target centre to the crystal surface, respectively. (x: before shaping, y: for a 4 mm gap between target chamber and end-cap, z: percentage of* 4π*).*

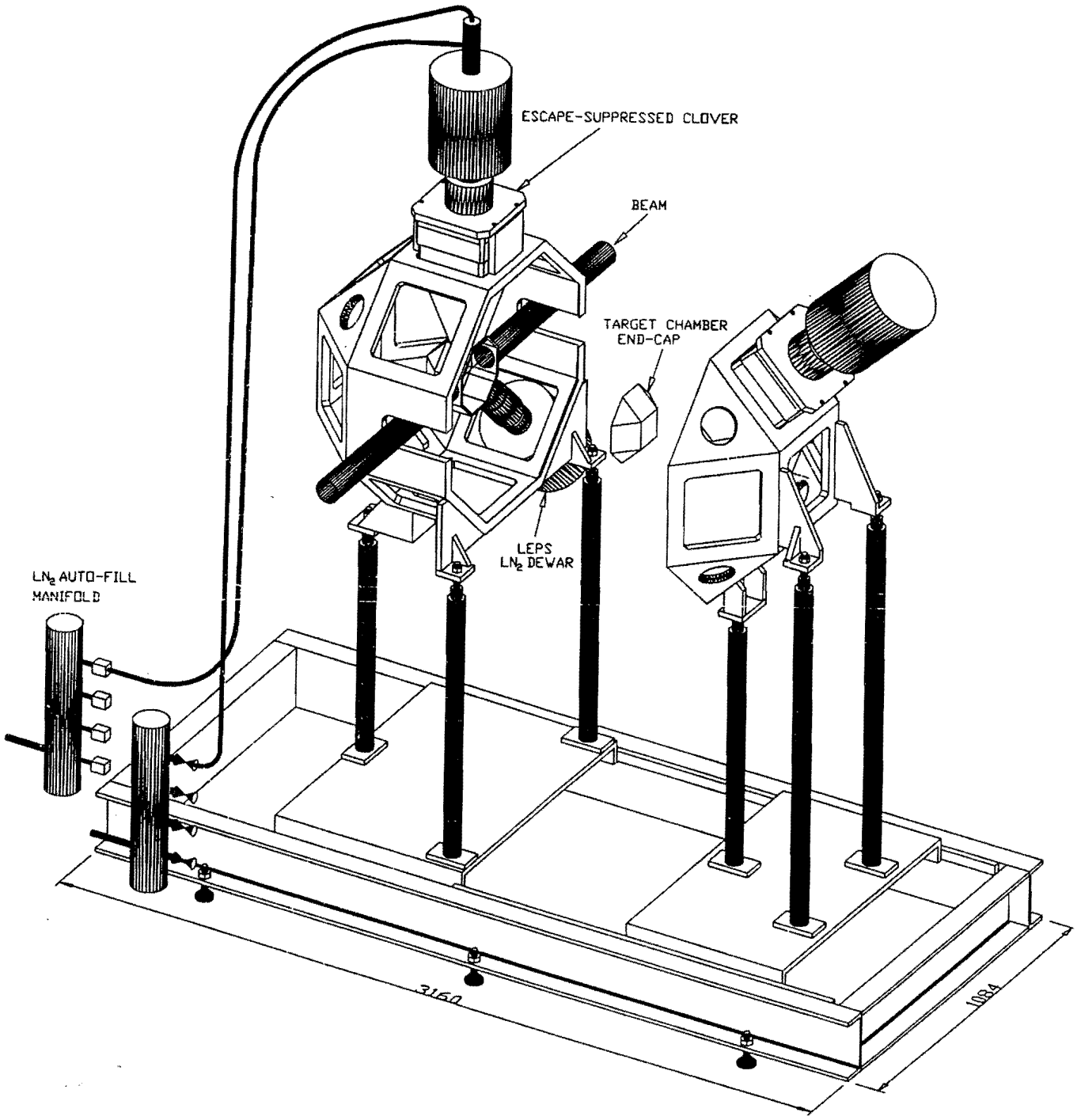

Figure 3.1: *A* drawing of the AFRODITE array-frame. Two Clovers in their BGO shields and a LEPS are shown [NAC98].

ADC (Analog-to-Digital Converter) in BPR (Bit Pattern Registers). These in turn were read by software via CAMAC.

A Clover detector consists of four crystal elements. The Clover elements at NAC are given labels to distinguish them from each other as shown in Figure 3.2.1. There is Clover element red, green, blue and black. Each element of the Clover can be assigned a bit value. For singles, the value of the bit pattern was set to 1 for the red element. For green it was set to 2, 4 for blue and 8 for black.

For add-back, the value of the bit pattern was set to 5 for the blue and red combination of elements and to 10 for the black and green, in the case of horizontal scattering. For vertical scattering, bit pattern values were set to 3 and 12 for the red and green and for the blue and black combinations of elements, respectively.

For the case where the value of the bit pattern is 1, 2, 4 or 8, spectra were accumulated as 'singles' events and summed for all the elements of the Clover detectors firing. For add-back, spectra were accumulated as horizontal events whenever the value of the bit pattern was 5 or 10, and as vertical events whenever the value of the bit pattern was 3 or 12.

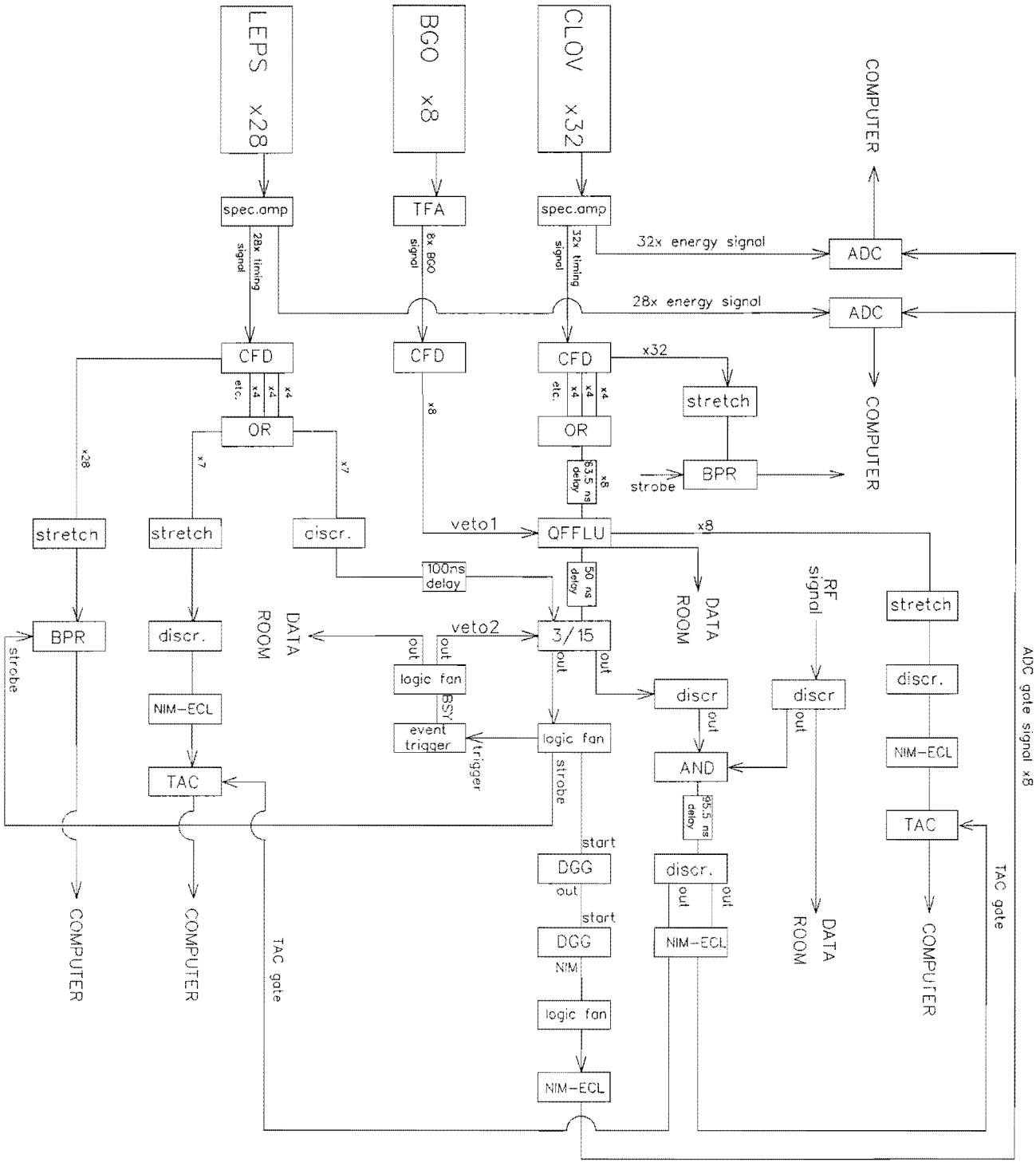

Figure 3.2: *A block diagram of the electronic set-up for the experiment.*

3.2.3 Measurements

The ^{164}Hf lines produced as by-products in the ^{142}Nd(^{27}Al, 4np) reaction were used to calibrate the polarimeter for its sensitivity to linear polarisation at these energies: 210 keV, 376 keV, 339 keV, 498 keV, 589 keV, and 635 keV.

In addition to this experiment, data were acquired out-of-beam using a ^{152}Eu source to perform energy calibration of the detectors, to measure the energy resolution and the relative and coincidence efficiencies of the detectors.

The CFD thresholds were set in the region of 50 keV above the noise at the time of the in-beam experiment.

Data were acquired under the condition that three out of fifteen detectors fire or register a pulse height. Singles and add-back events were accumulated for any element of the clover detector and for any pair of any adjacent clover elements firing, respectively, and was useful for the anisotropy and linear polarisation measurements.

All data were written in event-by-event mode on magnetic tape and were sorted off-line using the EVAL program [Hol79] which is a language for event analysis used at NAC. The gains of the amplifiers were adjusted to obtain an energy calibration of about 0.5 keV/channel for the Clover and the energy calibration was

performed using the RADWARE package [Rad88] at NAC . Peak fitting, background subtraction and gain adjustments were made using the RADWARE GF2 program. Detailed results are discussed in the following sections.

3.2.4 Characteristics Of The AFRODITE Detector

An ^{152}Eu radioactive source was used to evaluate the performance of the system in detecting unpolarised radiation. Subsequently, the energy resolution, the add-back and coincidence efficiencies and the geometric asymmetry of the detectors were measured. The noise level of the detectors was calculated to determine the effect it has on the deterioration of the energy resolution. The efficiency measurements were performed over the energy range 121 keV - 1408 keV.

3.2.4.1 Energy Resolution

The energy resolution, defined as the measure of the detector's ability to distinguish between closely-spaced lines in the spectrum, was measured. The energy resolution of the Clover detectors was measured by fitting Gaussian peaks of the ^{152}Eu source spectra. The peak fitting was done for both singles and add-back spectra to extract the width of the peaks. To get the

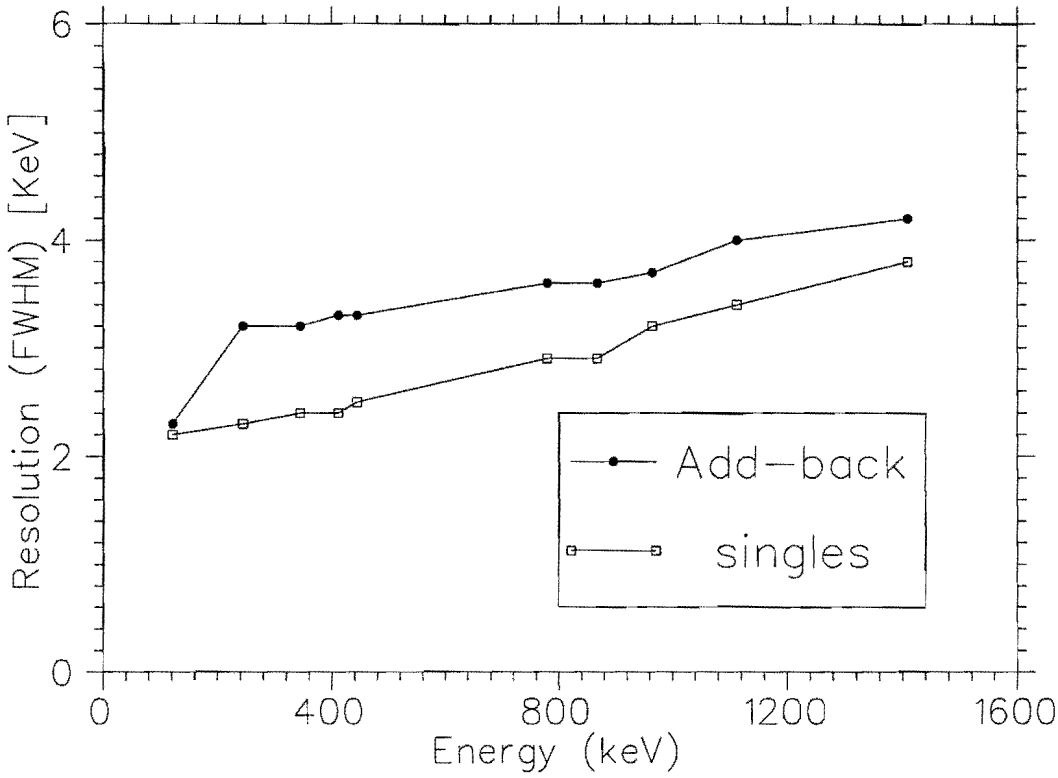

Figure 3.3: *Energy resolution of a Clover detector measured for singles and add-back events. In both cases the width increases with an increasing γ-ray energy.*

energy resolution of the detectors the width values were divided by 2 since the gain for Clovers is 0.5 keV/channel.

The relative energy resolution of a detector is defined as

$$R = \frac{\sigma}{E_\gamma} \tag{3.1}$$

where σ is the half width of a gaussian and is proportional to $E_\gamma^{1/2}$. If some energy, E_1, of the total energy, E_{tot}, incident on the detector is deposited on one element of the detector and E_2 is detected on the adjacent element such that $E_{tot} = E_1 + E_2$,

then $\sigma(E_1) = C_0 + C_1\sqrt{E_1}$ and $\sigma(E_2) = C_0 + C_1\sqrt{E_2}$ and

$$\sigma_{tot}^2 = \sigma_1^2 + \sigma_2^2 \tag{3.2}$$

Here σ_1 is the half width of the first element and σ_2 is that of the adjacent element of the detector. The total add-back energy resolution of the Clover detector is then given by $\Gamma_{tot} = 2\sigma_{tot}$, and

$$\Gamma_{tot}^2 = 4C_0^2 + 2C_1^2(E_1 + E_2) + 4C_0C_1(\sqrt{E_1} + \sqrt{E_2}) \tag{3.3}$$

using equation 3.2

Figure 3.3 shows plots of the resolution, Γ, against the radioactive source photon energy for singles and add-back events. A large difference between the resolutions of the singles and add-back events can be clearly seen in Figure 3.3 and in Table 3.1. The differences range from 0.1 keV at 122 keV to 0.6 keV at 1408 keV.

It should be mentioned that before the pulse heights resulting from Compton scattering were added from adjacent elements of the detector, they were energy calibrated and Doppler corrected. Doppler correction was done for each element of the Clover detector with β (the Doppler correction parameter) fixed to 0.0153. This value was obtained from $\beta = v/c$ with v being the measured recoil velocity of the residual ^{164}Hf nucleus and

c, the speed of light. The recoil velocity was determined from kinematics. Also, whenever a γ-ray is scattered between two adjacent elements of the detector, the average of the angles of the two elements (relative to the beam direction) was taken and used for Doppler correction. The addition of pulse heights in add-back mode will yield full energy events with a resolution that depends on the characteristics of both Clover elements and associated electronics. This should explain why for add-back the energy resolution is worse than the resolution measured for the singles events. For a germanium (either Ge(Li) or hyperpure-Ge) detector, measurements that have been done in other studies [Bea96, Jos97] give a resolution of 2.1 keV at 1.33 MeV for a ^{60}Co source and 1 keV at 122 keV for a ^{152}Eu source.

It can therefore be concluded that the resolution of the AFRODITE detectors we used is worse than that measured in the two references mentioned above. This deterioration in energy resolution can be attributed to a number of factors, which we discuss in the following sections.

3.2.4.1.1 Shaping Time Constant This is the amount of time it takes to have the pulse integrated by the Amplifier (the rising and the falling time of the pulse). If the pulse arrives within

Energy (keV)	**Resolution(Add-back)** (keV)	**Resolution(Singles)** (keV)
121.8	2.3	2.2
244.7	3.3	2.3
344.3	3.3	2.4
411.1	3.3	2.4
444.0	3.4	2.5
778.9	3.5	2.9
867.4	3.7	2.9
964.1	3.7	3.2
1112.1	3.9	3.4
1408.0	4.2	3.8

Table 3.1: Energy resolutions or width for add-back and singles events

any specified time it is accepted and digitised. If the pulse arrives before or after this time it is rejected. Too short or too long shaping time may worsen the resolution. All measurements were made using an amplifier(CAEN-16 channel) shaping time of 1 μs. This is a good shaping time for heavy ion experiments where one wants to process information faster to avoid the piling up of events. However, this time may be too short for source measurements and hence may lead to deterioration of the peak shape and the energy resolution of the detectors. A longer shaping time may be required for better resolution, provided the counting rate remains relatively low (about 2000 counts/second) during an in-beam experiment. A shaping time of 3 μs for the source is recommended at NAC for better results. [Jos97] used a shaping time of 6 μs in his analysis and obtained better results than those obtained in Table 3.1.

3.2.4.1.2 Detector Noise For a composite detector with k elements, the energy resolution is defined as:

$$\Gamma = \sum_{k} (N_k^2 + D_k^2 + L_k^2)^{\frac{1}{2}} \tag{3.4}$$

where N is the detector noise, and D and L represent the charge generating statistics and the charge losses due to impurities in the crystal, respectively. This means that for a four-element

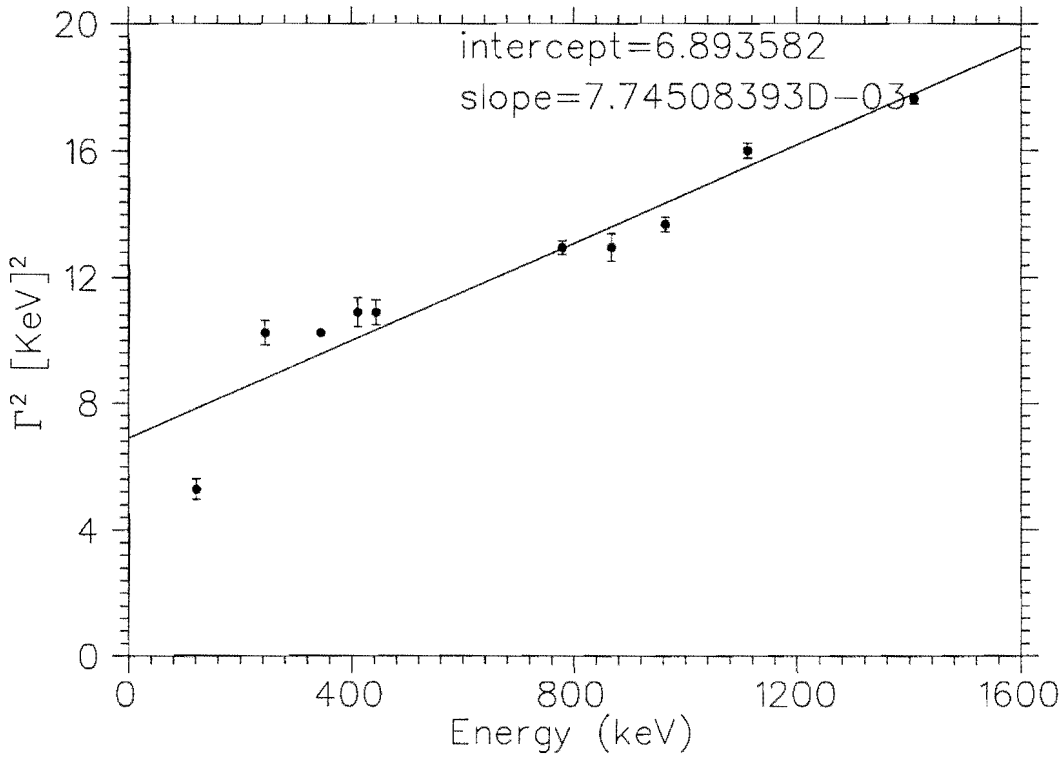

Figure 3.4: *A graph showing the relationship between the width and energy of γ-ray to determine the average detector noise between any two elements of a Clover.*

detector, in our case,

$$\Gamma^2 = N_1^2 + N_2^2 + 2.35^2 F \epsilon E_\gamma \tag{3.5}$$

with F, the Fano factor, equal to 0.1 for a germanium detector, ϵ the average energy required to create particle-hole in Ge, N_1 the noise level of the scatterer and N_2 that of the absorber [Sar95]. Using the slope from the graph in Figure 3.4 ($\epsilon = 11.5$ eV) and equation 3.5 above, the average noise for two elements (absorber and scatterer) of the detector was calculated to be 1.86 keV. The solid line is a least-square fit to the data points. The assumption made is that in equation 3.5 above, $N_1 = N_2$ since we do not know in our case which crystal is the scatterer and which is the absorber.

In [Sar95], detector noise level was measured and a value of 0.29 keV for the scatterer and 0.47 keV for the absorber was obtained. Our results show that there is an undesirably large noise level in our detectors.

3.2.4.2 Relative or Add-back Efficiency

The relative efficiency of the polarimeter also known as add-back efficiency, is defined for a composite detector as $\frac{N_\parallel}{N_s}$ or $\frac{N_\perp}{N_s}$. $N_\parallel$ and $N_\perp$ represent the number of photons scattered horizontally and vertically between two adjacent elements of a detector, re-

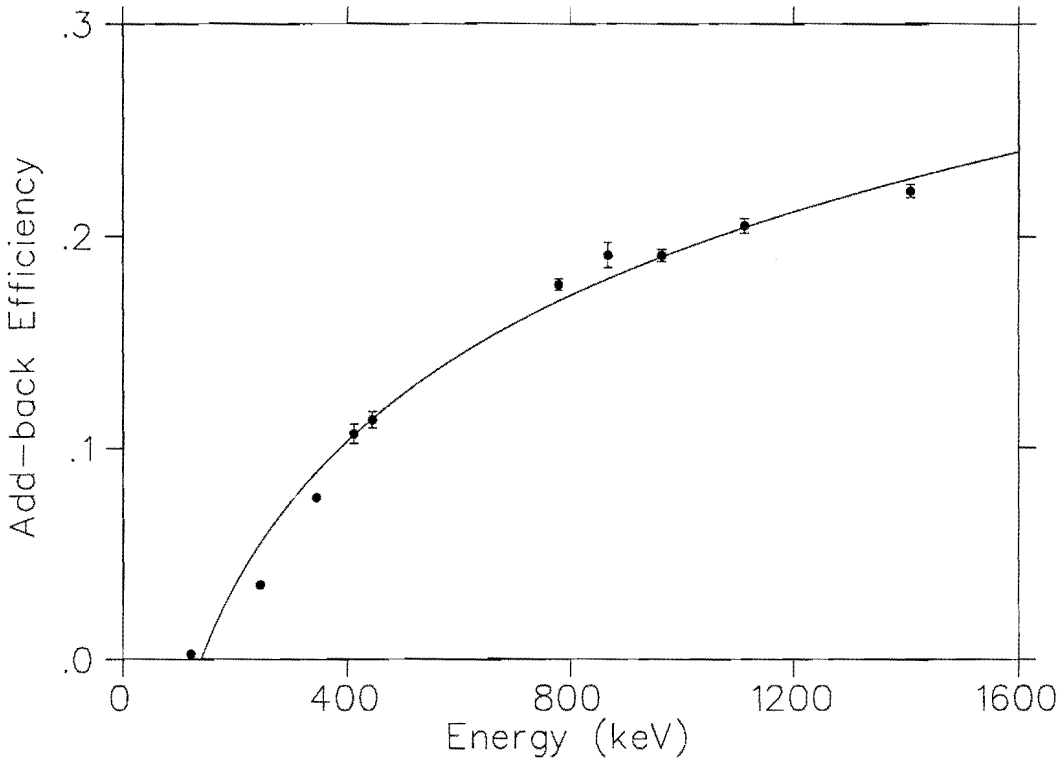

Figure 3.5: *The probability of having Compton scattering between any two adjacent elements of a Clover detector.*

spectively and N_s those totally absorbed in one element. The relative efficiency $(\frac{N_\perp}{N_s})$ was measured and Figure 3.5 shows a plot of the add-back to singles ratio against the γ-ray energy. It is noted that the Compton scattering probability increases with an increase in photon energy. Saturation should be reached at higher energies [Lis78].

The solid line fitted to the data points for both add-back and the coincidence efficiency is a quadratic function.

Energy(keV)	Relative Efficiency	Coincidence Efficiency
121.8	0.002	0.005
244.7	0.04	0.073
344.3	0.08	0.155
411.1	0.10	0.212
444.0	0.12	0.232
778.9	0.18	0.357
867.4	0.18	0.374
964.1	0.19	0.383
1112.1	0.20	0.408
1408.0	0.22	0.443

Table 3.2: Tabulation of γ-ray energy, relative (ratio of add-back and singles events) and coincidence efficiency ϵ_{coinc} to examine the performance of the polarimeter.

3.2.4.3 Coincidence Efficiency

The coincidence efficiency is defined as

$$\varepsilon_{coinc} = \frac{N_{\perp} + N_{\parallel}}{N_s} \tag{3.6}$$

where N_s is the total number of singles events. Figure 3.6 shows the relationship between ε_{coinc} and the γ-ray energy. Equation 3.6 gives the ratio of the number of events scattered in the horizontal and vertical directions relative to the beam direction to the total number of singles events.

The coincidence efficiency, ε_{coinc}, is very useful for the calculation of the figure-of-merit which is usually quoted when comparing the performance of Compton polarimeters. Results for the measured ε_{coinc} and relative efficiency are shown in Table 3.2 above. The coincidence efficiency, ε_{coinc}, has been found to be approximately 40% at 1199 keV for a Clover detector at NAC.

3.2.4.4 Geometric Asymmetry

The anisotropy associated with the geometry of the polarimeter was measured for one detector using equation 2.9 and found to be close to zero. This shows that a Clover detector is highly symmetric. The scaling factor, $a(E\gamma)$, used to modify equation 2.9 in order to correct for efficiency, is close to one and does not

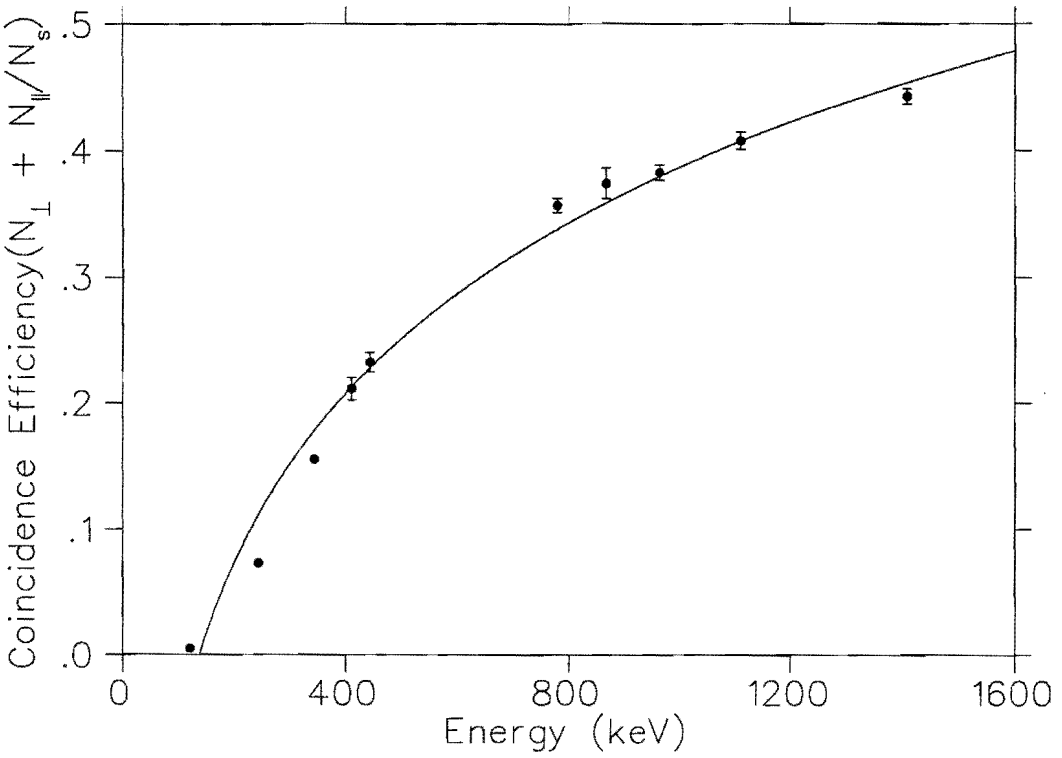

Figure 3.6: *The probability of having γ-rays detected in coincidence in any two adjacent elements of a Clover detector.*

Energy(keV)	A	$a(E_\gamma)$
121.8	0.024	0.954
244.7	−0.029	1.059
344.3	−0.012	1.025
411.1	0.011	0.979
444.0	−0.024	1.050
778.9	−0.008	0.985
867.4	0.020	0.958
964.1	−0.001	1.003
1112.1	0.007	0.987
1408.0	0.002	0.996

Table 3.3: *Anisotropy associated with the geometry of the detector and the scaling factor $a(E_\gamma)$ to correct for it.*

show any dependence on energy. Table 3.3 shows the anisotropy, A, measured for unpolarised radiation using a ^{152}Eu radioactive source. This anisotropy is expected to vanish for unpolarised radiation but does not due to slightly different efficiencies between adjacent elements of the polarimeter in detecting γ-rays. To correct for this, a normalisation factor, $a(E_\gamma)$, can be used to modify equation 2.9 which now becomes

$$A(\eta) = \frac{a(E_\gamma)N_\perp - N_\parallel}{a(E_\gamma)N_\perp + N_\parallel} \tag{3.7}$$

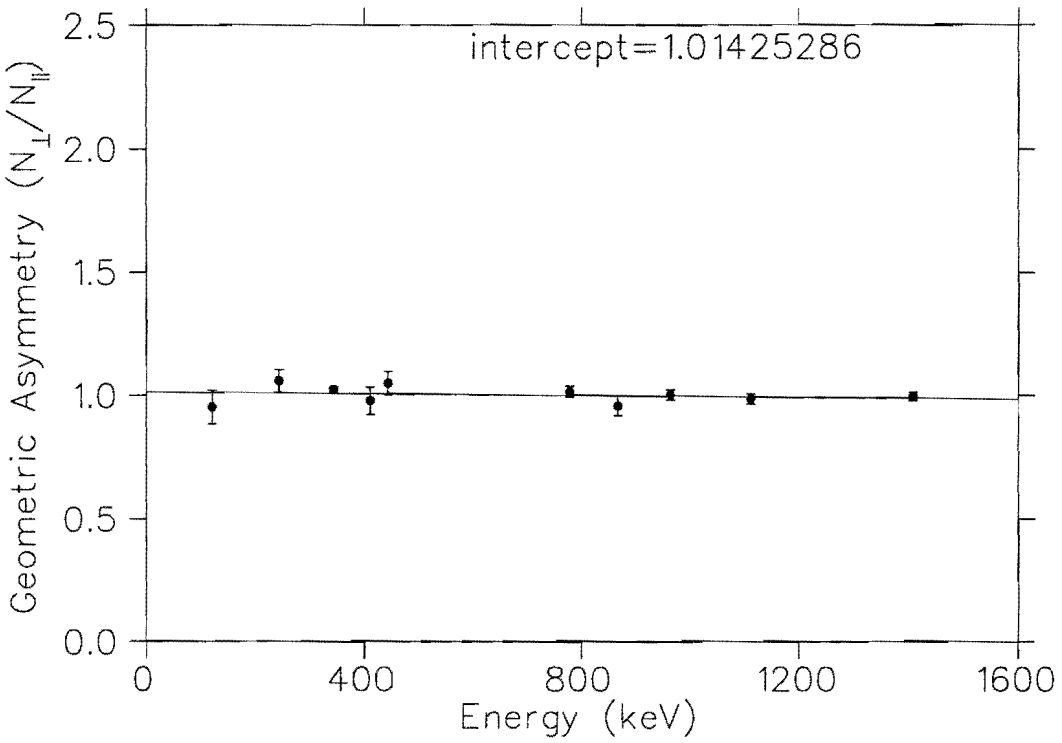

Figure 3.7: *A graph of geometric anisotropy, $a(E_\gamma)$, as a function of γ-ray energy for a Clover detector.*

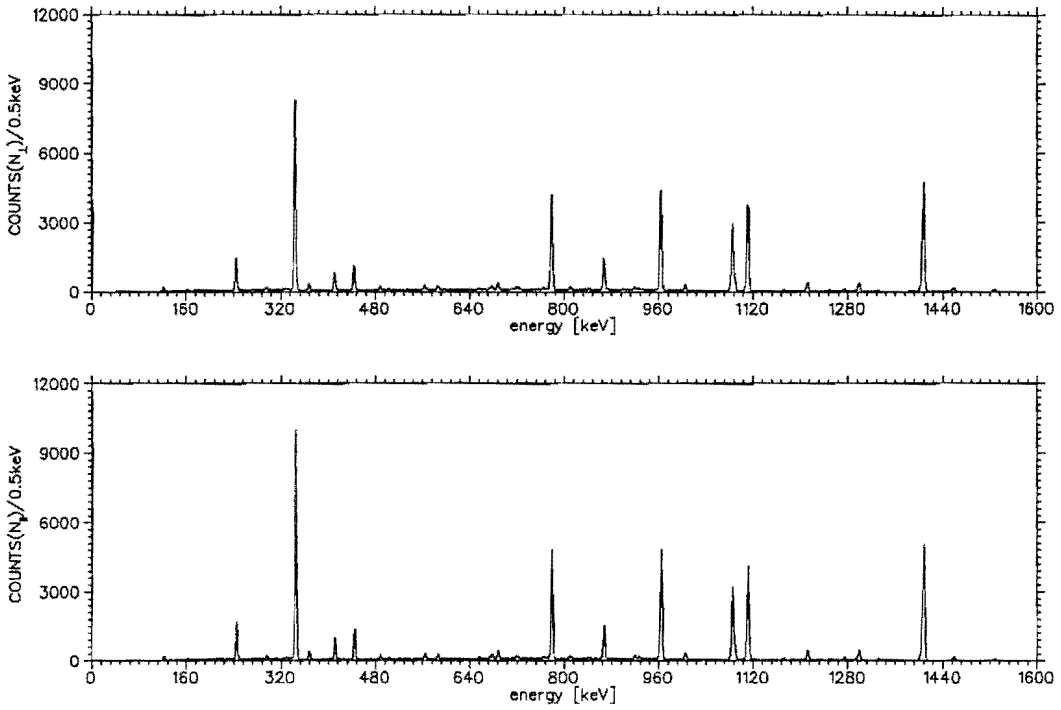

Figure 3.8: *Measured add-back ^{152}Eu spectra used for detection efficiency calibration. The upper part is the vertical spectrum and the lower part is the horizontal spectrum.*

where

$$a(E_\gamma) = \frac{N_{||}}{N_\perp} \tag{3.8}$$

for unpolarised radiation.

Figure 3.8 shows the vertical $N_\perp$ and the horizontal $N_{||}$ spectra for a source of unpolarized γ-rays form ^{152}Eu. The normalisation factor, $a(E_\gamma)$, is nearly equal to 1 (= 1.01) for one Clover detector as can be seen in Figure 3.7 and in Table 3.3 and does

not display any energy dependence. This also demonstrates the high degree of symmetry the Clover detector possesses.

When analysing the source spectra in Figure 3.8 after summing up spectra for three different Clover detectors at 90°, it was found that for $a(E_\gamma) = 1$, $A(\eta)$ in equation 3.7 does not vanish as expected for the source but ranges between -2.2% and 3.0%. However, when $a(E_\gamma) = 0.95$, $A(\eta)$ is reduced to 0.5%. A normalisation factor of 0.95 was thus used throughout.

Chapter 4

ANALYSIS OF POLARISATION WITH AFRODITE

A polarimeter can be geometrically calibrated and $a(E_\gamma)$, the asymmetry associated with the geometry of the polarimeter, can be measured using unpolarised radiation emitted by a ^{152}Eu radioactive source. The polarimeter can also be calibrated for its sensitivity to linear polarization using well known $E2$ transitions. Seven Clover detectors were used to acquire data. Four of these detectors that are at 90° were gated by seven ^{164}Hf transitions, selected mainly from the ground state band of ^{164}Hf. The ^{164}Hf level scheme is shown in Figure 4.1. Spectra were updated for any of the seven lines satisfying the gate and for any

of the four detectors firing. All the transitions used (210.8 keV, 376.4 keV, 498.2 keV, 339.0 keV, 583.7 keV, 635.6 keV and the 566.9 keV linking transition) are $E2$ transitions. The spectra from three of the four Clover detectors at 90° were summed to improve statistics, and only these detectors were used for polarisation measurements (the fourth detector had a faulty element). The angular distributions of γ-rays were constructed from measurements at the angles of 45° and 135°, and at 90°. Data from all detectors at 45° and 135° were also summed to improve statistics. The angular distribution coefficients were extracted using equation 2.2 in Chapter Two. By taking the difference between events scattered horizontally and those scattered vertically and normalizing by the sum, the anisotropy of γ-rays was determined. This information combined with the angular distributions associated with each transition enabled the determination of the linear polarisation of the ^{164}Hf and ^{165}Ta γ-rays.

4.1 SENSITIVITY CALIBRATION

An internal calibration of the polarimeter for its sensitivity to linear polarisation was done using well-known $E2$ transitions

(210.8 keV, 376.4 keV, 498.2 keV, 339.0 keV, 583.7 keV, 635.6 keV and the 566.9 keV) of ^{164}Hf most of which are selected from the ground state band of ^{164}Hf as shown in Figure 4.1. It should be mentioned that the calibration was achieved using a heavy ion reaction rather than a proper (p, γ) reaction normally used for calibrating a polarimeter. ^{164}Hf levels were populated in-beam in the ^{142}Nd(^{27}Al, 4np) reaction at the beam energy E of 150 MeV. The spectra, gated and ungated, were analysed to test the technique.

4.1.1 Analysis Of Ungated Spectra

After correcting for efficiencies, a detailed data analysis of the experimental results was made by considering the difference $(N_{\perp} - N_{\parallel})$ spectrum. Measurements were made first using ungated spectra as a test. Figure 4.2 shows the ungated horizontal γ-ray spectrum for horizontally scattered events, the ungated vertical spectrum for vertically scattered events, and the difference spectrum showing which transitions are polarised and also giving the sign of their polarisation. Vertical and horizontal counts shown in Figure 4.2 were acquired by taking the sum of counts in all the detectors at 90°, and were added together separately.

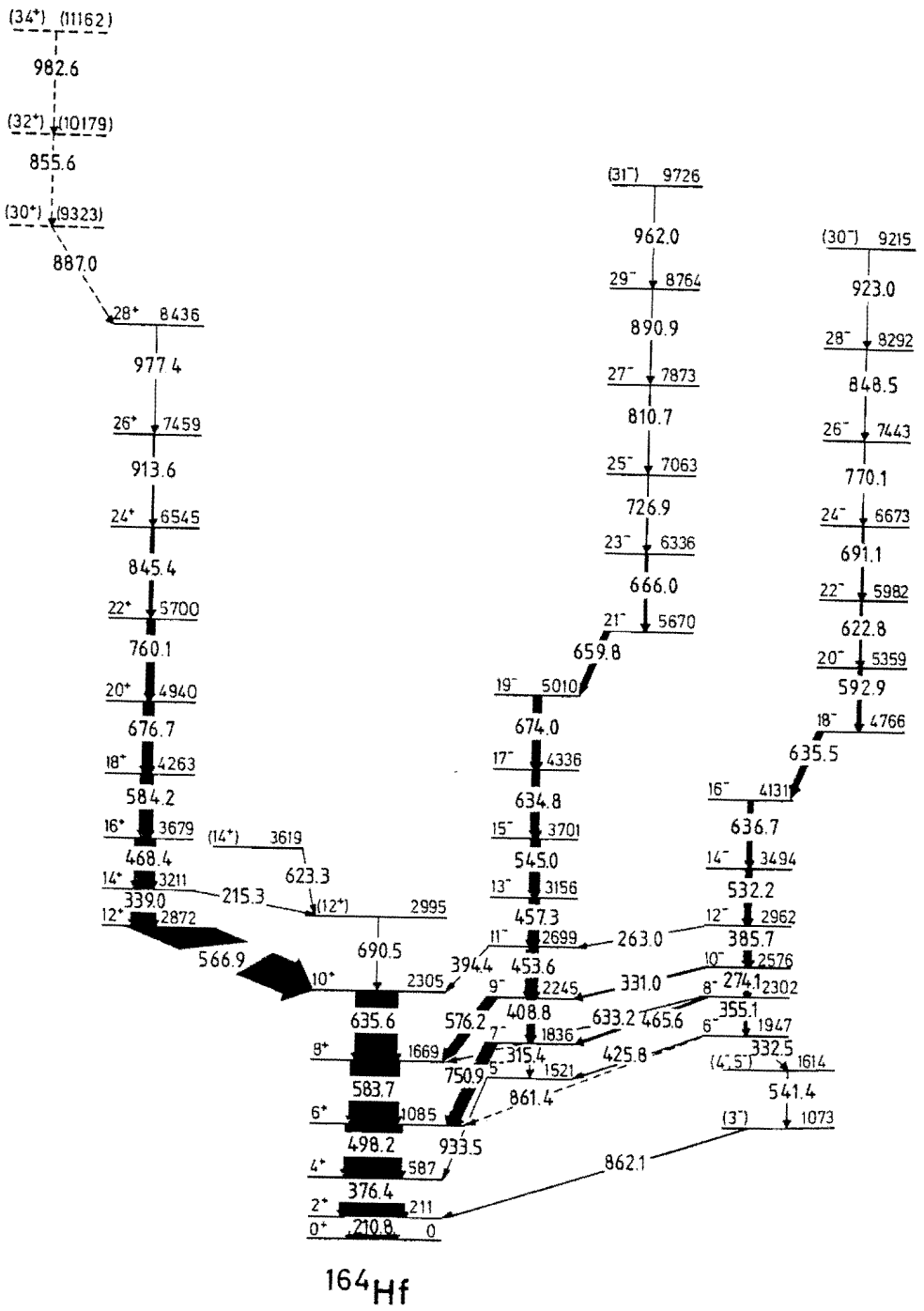

Figure 4.1: *A level scheme diagram of ^{164}Hf. γ-rays selected mainly from the ground state band of ^{164}Hf were used to calibrate the polarimeter.*

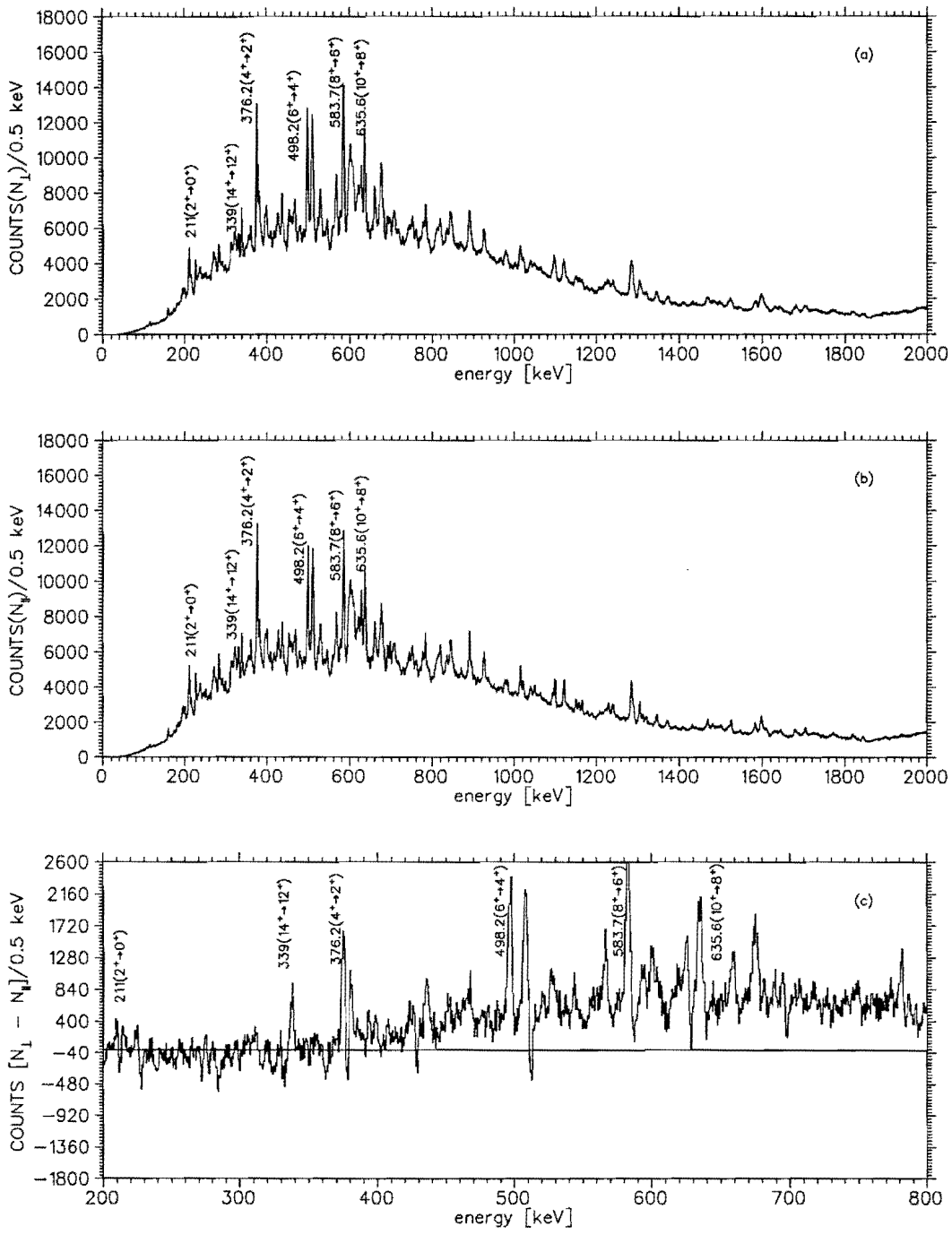

Figure 4.2: *a) and b) : The total projection spectra of vertically and horizontally scattered events, respectively. c) : Difference $N_{\perp} - aN_{||}$ spectrum showing which ^{164}Hf γ-lines are polarised.*

In the difference spectrum c) in Figure 4.2, the 376.4 keV γ-ray appeared to be a doublet. Since no γ-ray was found to be in coincidence with the 376.4 keV γ-ray in ^{164}Hf level scheme, thus leaving no basis for believing this observation, the cause of this effect was investigated. Other dips which also appeared like peaks were observed and it was found that they were due to a slight shift in γ-ray energy. The Gains of the spectra were adjusted using Radware package, GF2, to solve the problem [Rad88]. The dips disappeared after the gain corrections and the 376 keV γ-line appeared as a single peak, dismissing the notion that it could be a doublet.

The lesson is that care should always be taken when taking a difference between horizontally and vertically scattered events as the resulting spectrum may yield spurious effects and misleading results if energy calibration or gain matching or both have not been done properly.

After correcting the gains, the ungated spectra (vertical and horizontal) were background subtracted and efficiency corrected and the difference $N_\perp - aN_\parallel$ where a is $\frac{N_\perp}{N_\parallel}$ was taken as shown in Figure 4.3. The dips were successfully removed from the spectrum. It can be clearly seen from the difference spectrum that all the ^{164}Hf lines are polarised with the sign of their polarisation

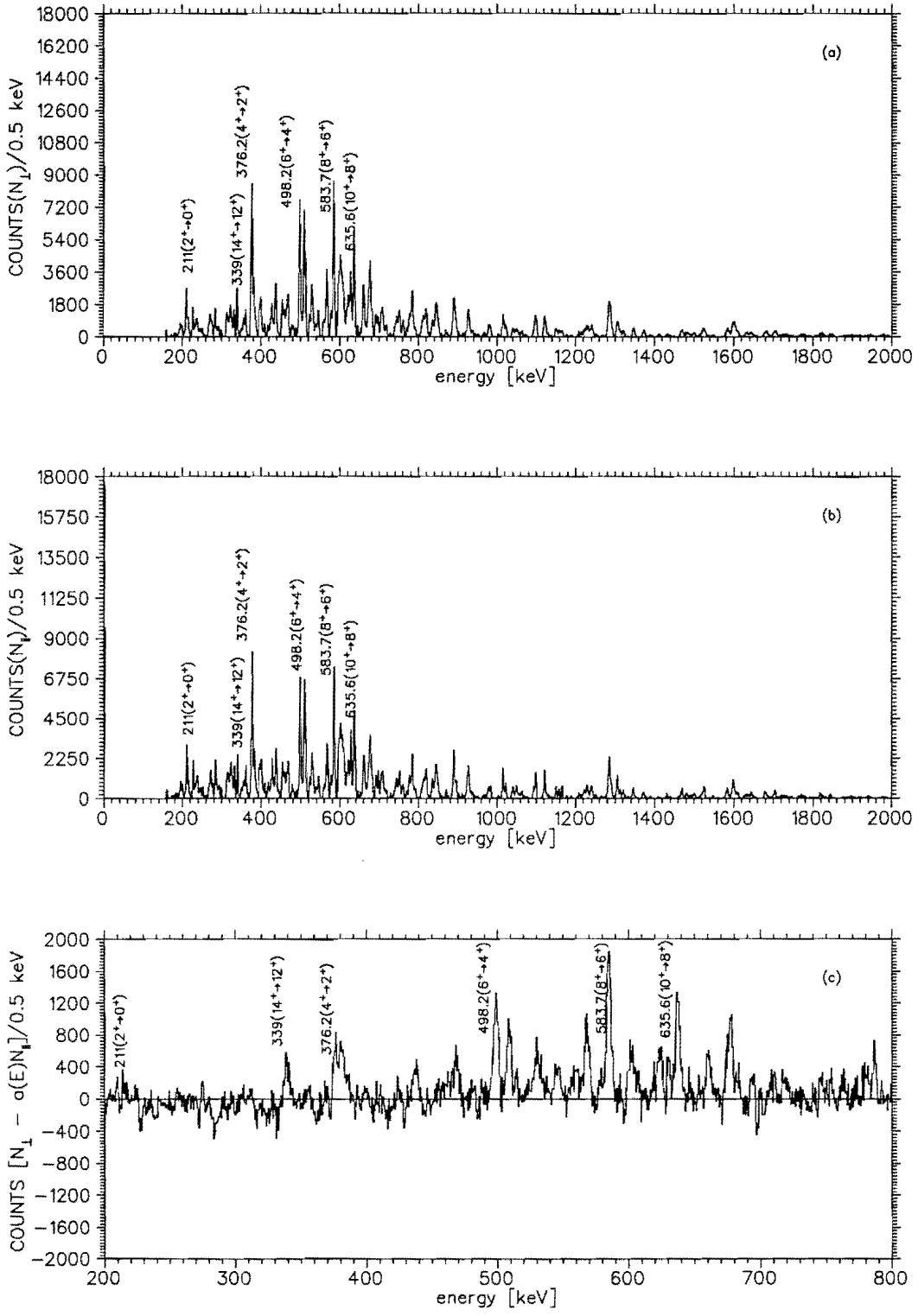

Figure 4.3: *a) and b) : The ungated and background subtracted total projection spectra of vertically and horizontally scattered events, respectively. c) : Difference $N_\perp - aN_{||}$ spectrum corrected for efficiency, showing which ^{164}Hf γ-lines are polarised.*

being positive.

These preliminary results clearly show that the technique works. However, cleaner spectra were needed to get more precise results in order to support this view. This was achieved by setting the gates on our spectra by software.

4.1.2 Analysis Of Gated Spectra

For analysis of gated spectra, add-back spectra were acquired by gating in the singles spectra by seven ^{164}Hf lines which were produced as by-products from the ^{142}Nd(^{27}Al, 4np) reaction. Gating was done to clean up the spectra. The same procedure employed to analyse ungated data in Section 4.1.1 above was used here as well. The difference spectrum is shown in Figure 4.4.

As discussed in Chapter Two, γ-rays of electric ($E1$ or $E2$) character that have their electric vectors in the reaction plane (a plane defined by the beam direction and the direction of the scattered γ-ray), are scattered vertically in the crystal (in the direction normal to the reaction plane) and yield a positive value for anisotropy. On the other hand, γ-rays of magnetic ($M1$ or $M2$) character that have their electric vectors in the plane normal to the reaction plane, are scattered horizontally in the crystal (in the direction parallel to the reaction plane)

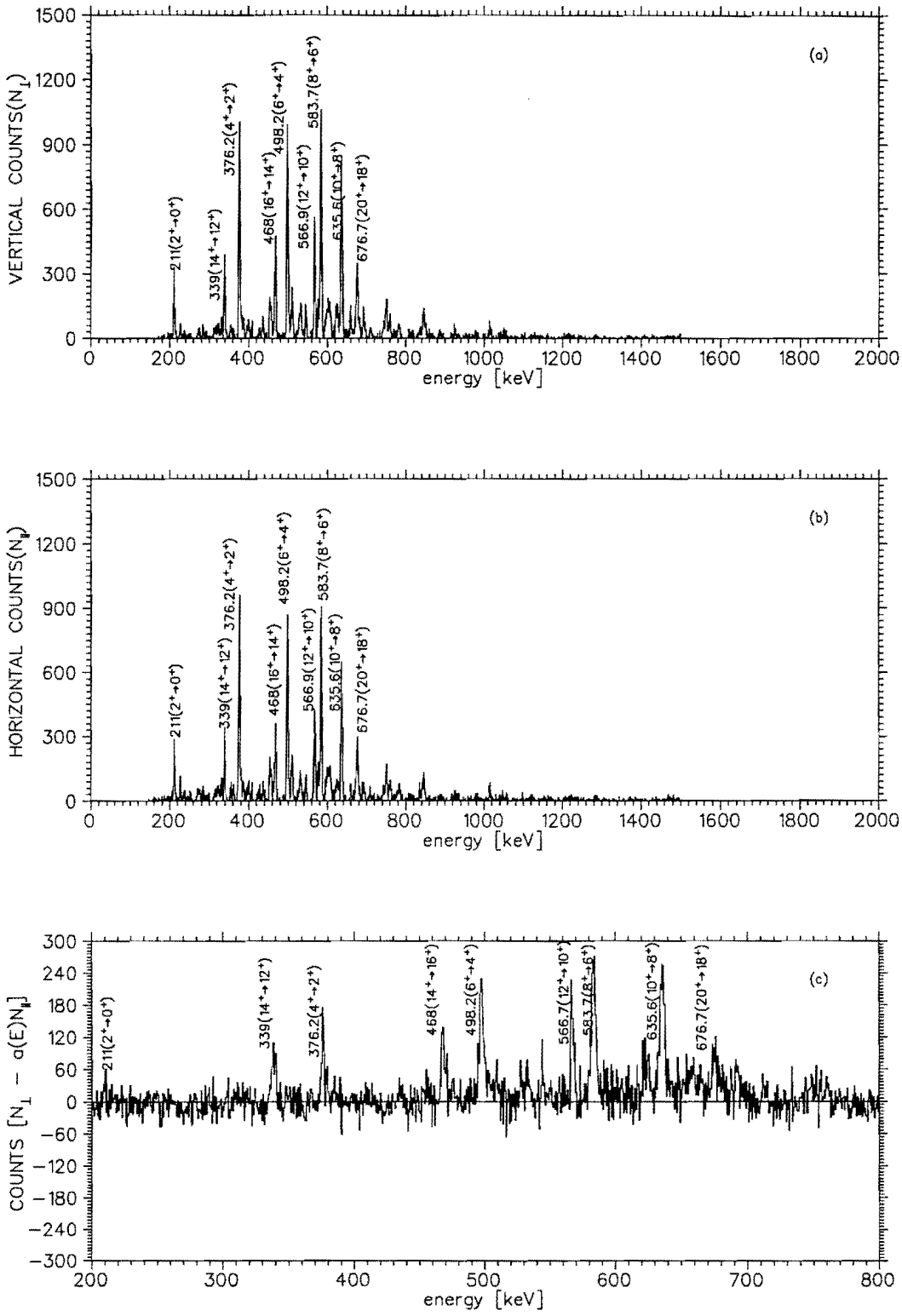

Figure 4.4: *a) and b) : The gated and background subtracted total projection spectra of the vertically and horizontally scattered events, respectively. c) : Difference $N_\perp - aN_{||}$ spectrum corrected for efficiency, showing which ^{164}Hf γ-lines are polarised.*

Energy(keV)	$(N_\perp)$	$(N_\parallel)$	$A(\frac{N_\perp - aN_\parallel}{N_\perp + aN_\parallel})$
210.8	2272 ± 48	2219 ± 47	0.0374 ± 0.0474
339.0	3181 ± 56	2583 ± 51	0.1290 ± 0.0164
376.4	9001 ± 95	8503 ± 92	0.0542 ± 0.0143
489.2	9134 ± 96	7475 ± 87	0.1253 ± 0.0098
566.9	5039 ± 71	4143 ± 64	0.1229 ± 0.0137
583.7	10340 ± 102	8305 ± 91	0.1344 ± 0.0091
635.6	8240 ± 91	6243 ± 79	0.1629 ± 0.0093

Table 4.1: *Anisotropy measurements from the difference between the intensity of events scattered vertically ($N_\perp$) and that of events scattered horizontally ($N_\parallel$) for ^{164}Hf nucleus. The anisotropy, $A(\theta)$, is normalised to the total scattered events.*

and yield a negative value for anisotropy. It can be clearly seen from the difference spectrum that the ^{164}Hf γ-rays are polarised, all appearing with positive counts and thus corresponding to electric transitions. All the intense γ-lines are $E2$ transitions. We could not find strong magnetic transitions in ^{164}Hf. However, these results combined with those shown in Section 4.1.1 and in Figure 4.4 reveal that the technique works.

The intensity of the γ-rays in add-back mode was determined using a Radware fitting program, GF2, and their anisotropy calculated using equation 3.7. Table 4.1 shows the values for anisotropy and their corresponding errors. The error in anisotropy

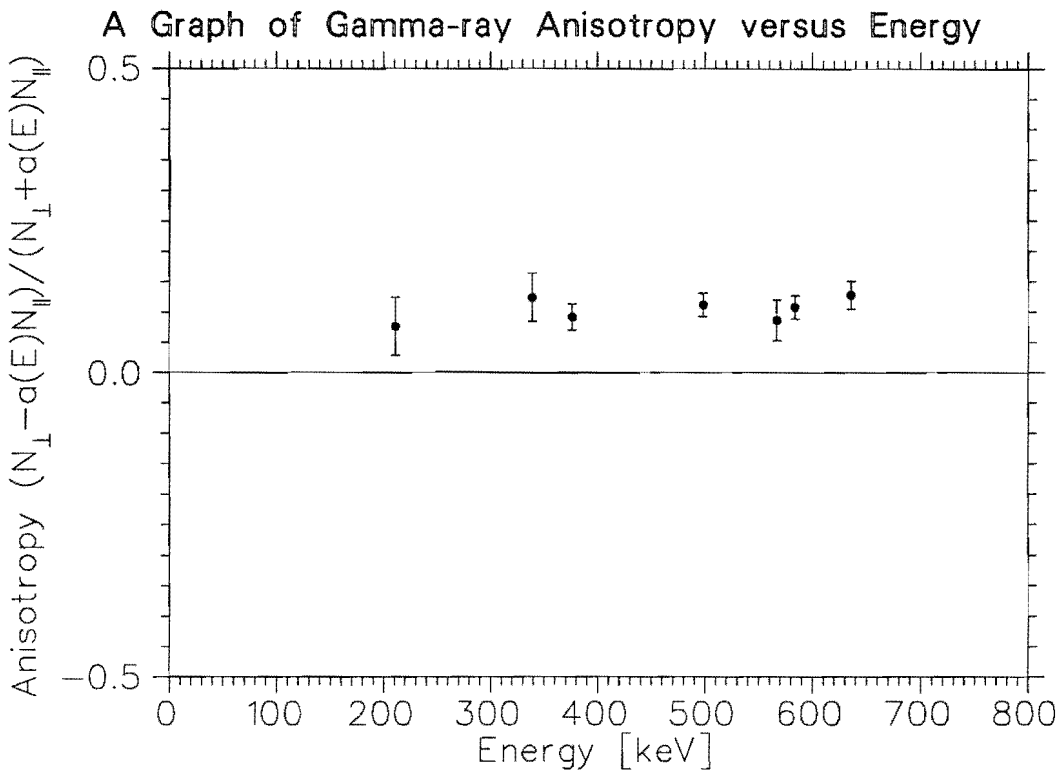

Figure 4.5: *A plot of anisotropy versus energy for ^{164}Hf γ-rays .*

ranges from 6% at 635.6 keV to 127% at 210.8 keV. The point at 210.8 keV is definitely inaccurate as the error of the value of A at this energy is bigger than the value of A.

As shown in Figure 4.5, all the ^{164}Hf lines have positive anisotropy and subsequently a positive value for polarisation, confirming spectrum c) in Figure 4.4.

4.1.3 Angular Distributions

The angular distribution coefficients were calculated using equation 2.2. Because the AFRODITE detector array has its detec-

E_γ(keV)	a_2	A(90°)
339.0	0.2230 ± 0.0230	0.1290 ± 0.0164
376.4	0.0300 ± 0.0016	0.0542 ± 0.0143
498.2	0.2330 ± 0.0160	0.1253 ± 0.0098
566.9	0.2980 ± 0.0277	0.1229 ± 0.0137
583.7	0.3310 ± 0.0206	0.1344 ± 0.0091
635.6	0.3750 ± 0.0267	0.1629 ± 0.0093

Table 4.2: *Measured angular distribution coefficients for selected γ-rays associated with decay of high spin states of ^{164}Hf.*

tors located only at 45°, 135° and at 90° relative to the beam direction, a_4 could not be calculated and was assumed to be zero. Nevertheless a_4 is very close to zero for quadrupole radiation and its omission will not have a considerable effect on our results. Figure 4.6 shows gated spectra of singles events at 45°, 135° and at 90° relative to the beam direction. These spectra were used to determine the angular distribution coefficients. We therefore expect a pure quadrupole transition to have a maximum intensity at 45° and 135° and a minimum intensity at 90°.
As can be seen in Figures 4.7 and 4.8 and in Table 4.2, the sign of the angular distribution coefficients is positive for a quadrupole (e.g. M2 or $E2$) transition.

Angular distribution coefficients were extracted as described in

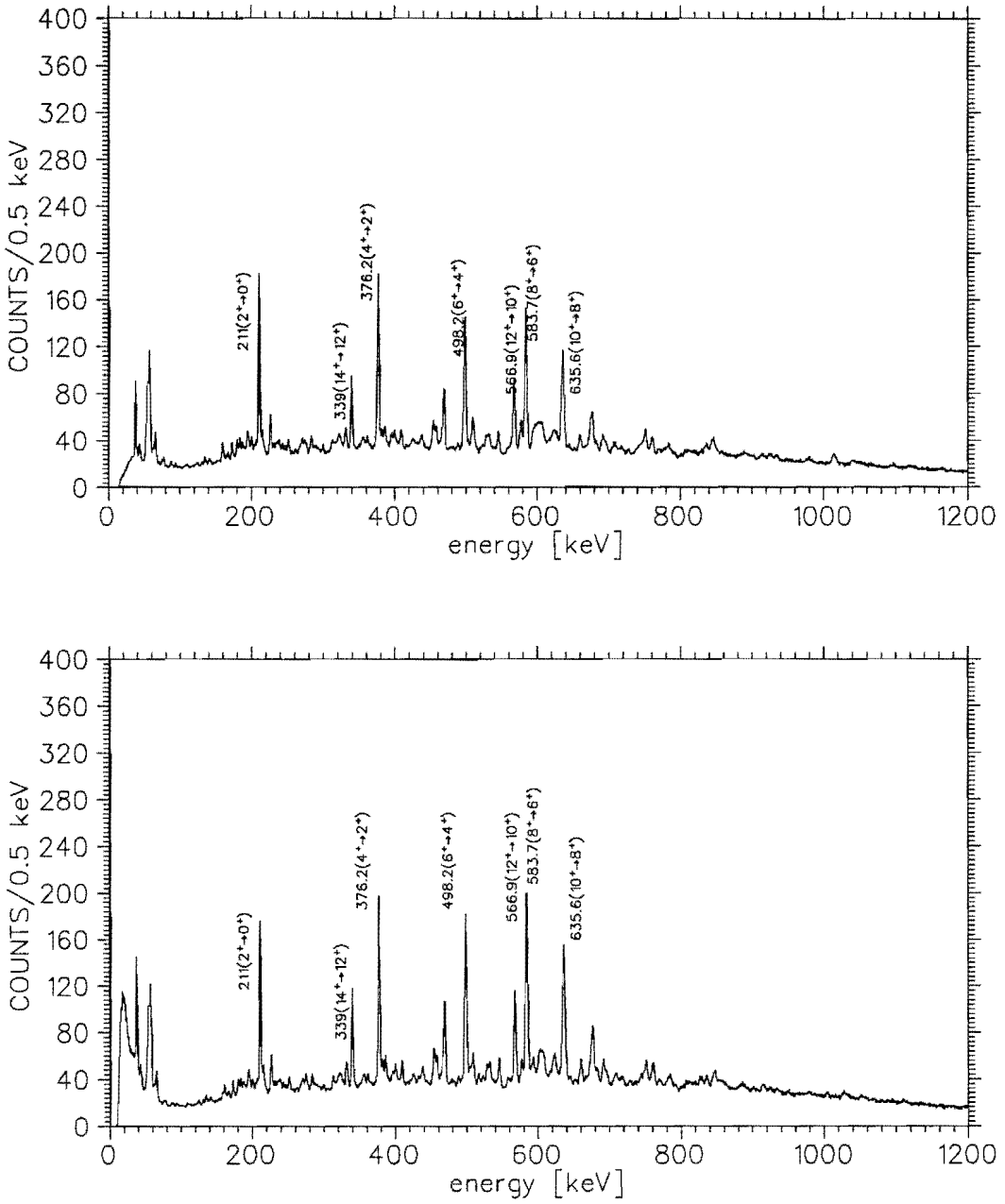

Figure 4.6: *Upper part: singles spectrum for detectors at* 90° *relative to the beam. Lower part: singles spectrum for detectors at* 45° *and* 135° *relative to the beam.*

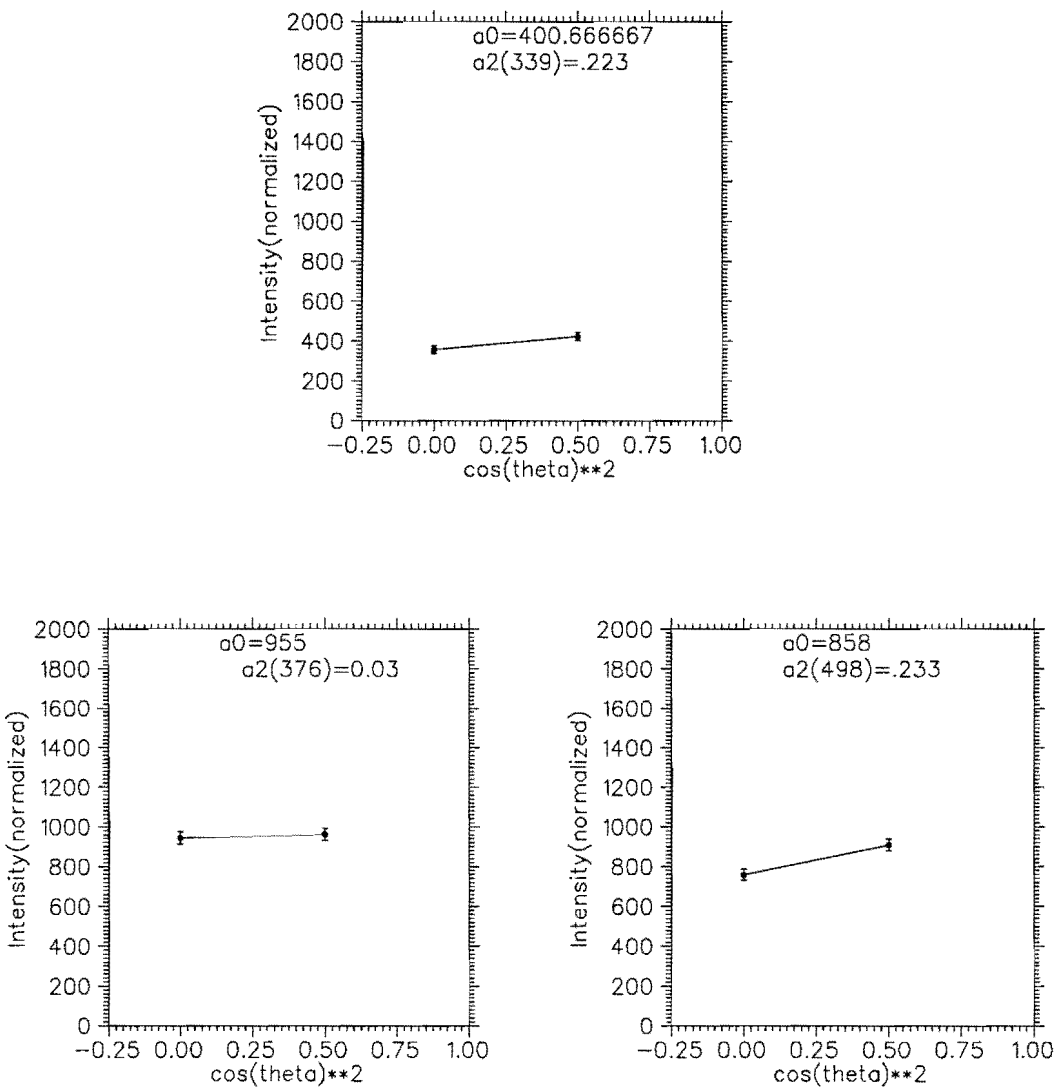

Figure 4.7: *Plots of normalised γ-ray intensity versus $\cos^2\theta$ for the determination of angular distribution coefficients for the ^{164}Hf nucleus. The energies, in keV, of the γ-rays are enclosed in brackets.*

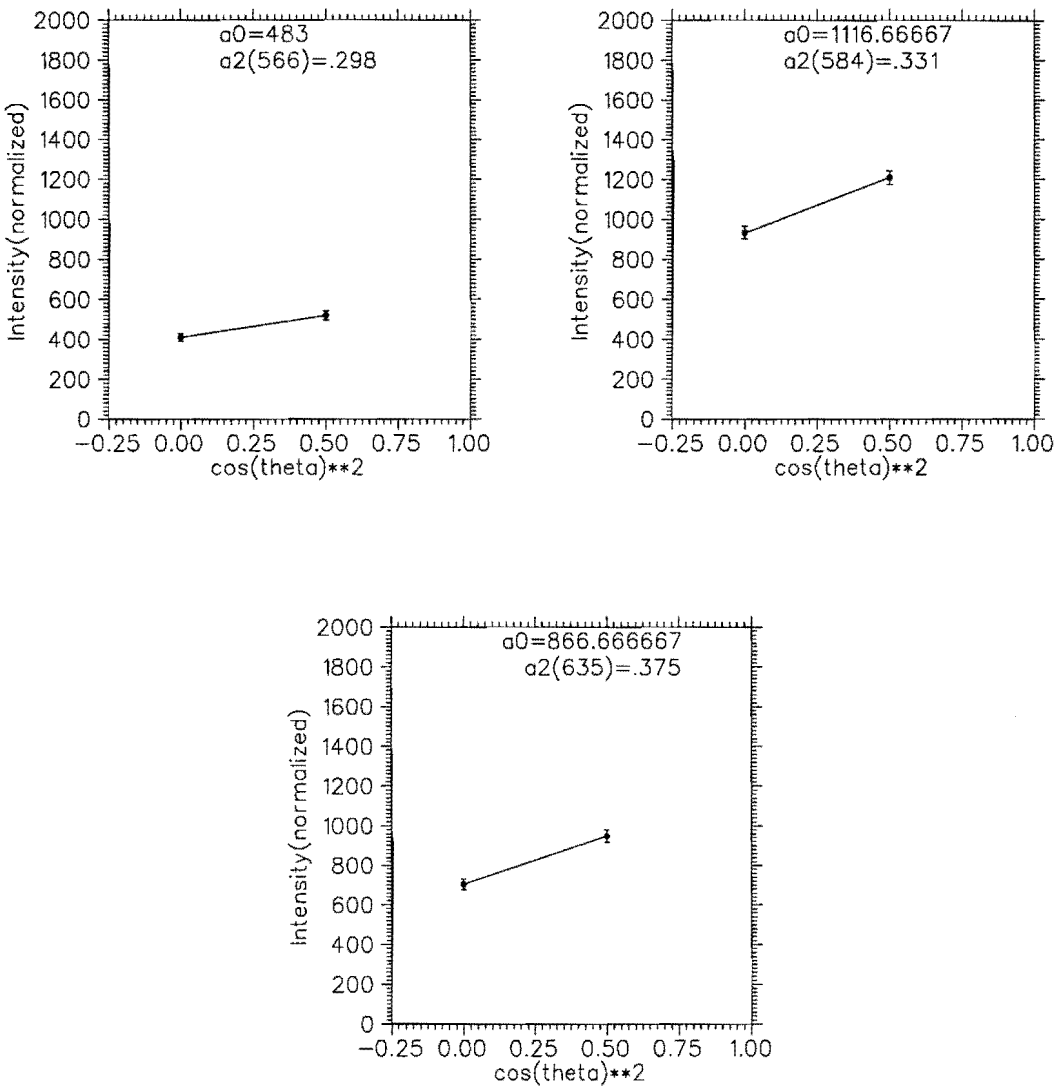

Figure 4.8: *Plots of normalised γ-ray intensity versus $\cos^2\theta$ for the determination of angular distribution coefficients for the ^{164}Hf nucleus. The energies, in keV, of the γ-rays are enclosed in brackets.*

Chapter Two. Equation 2.2 was fitted to the data in Figures 4.7 and 4.8and the curves shown in the figures are the results of these fits. The extracted values of the angular distribution coefficients were substituted in the formula

$$P(\theta = 90°) = \pm\frac{3a_2 + 1.25a_4}{2 - a_2 + 0.75a_4} \tag{4.1}$$

in order to calculate the linear polarisation of the γ-rays. Using calculated values of polarisation and the measured anisotropy of γ-transitions the polarisation sensitivity, Q, was calculated from equation 2.13 in Chapter Two. The deduced values of the linear polarisation are shown in Table 4.3, along with the polarisation sensitivity of the detector. The results are plotted in Figure 4.9. The data points have been fitted using equation 2.22 in Chapter Two and appear to follow a decrease in Q as E increases, as expected. The b_1 and b_0 shown in Figure 4.9 are the parameters X and Y in equation 2.22. These results show that the polarimeter is sensitive to linear polarisation, however, over a very small energy region of 339 keV - 635 keV. In [Jon95], the polarimeter was calibrated and its sensitivity to polarisation measured over the energy range 197 keV - 1368 keV. Our values for Q seem to be slightly higher compared to those obtained elsewhere. For an example, in [Jon95] a value of 0.34(9) at 197

E_γ(keV)	P(90°)	Q(E_γ)
339.0	0.3765 ± 0.0510	0.3428 ± 0.0638
376.4	0.0457 ± 0.0030	–
498.2	0.3956 ± 0.0274	0.3168 ± 0.0331
566.9	0.5253 ± 0.0501	0.2340 ± 0.0336
583.7	0.5950 ± 0.0385	0.2259 ± 0.0211
635.6	0.6923 ± 0.0512	0.2354 ± 0.0225

Table 4.3: *A table showing polarisation and polarisation sensitivity values for selected γ-rays associated with decay of high spin states of ^{164}Hf.*

keV was obtained whereas we have obtained more or less the same value at a higher energy of 339.0 keV. Big error bars on this point at 339.0 keV as shown in Figure 4.9 suggest that this point is not precise (it has about 18% error). However, within experimental margin of error it is acceptable.

The value of Q at 376 keV has been omitted since it is so small and this could be because of heavy side feeding.

4.2 APPLICATION OF THE TECHNIQUE TO ^{165}TA DATA

The polarimeter has been successfully applied to γ-rays associated with the decay of high-spin states in ^{165}Ta for polarisation measurements. Data were acquired from the ^{142}Nd(^{27}Al, 5n)

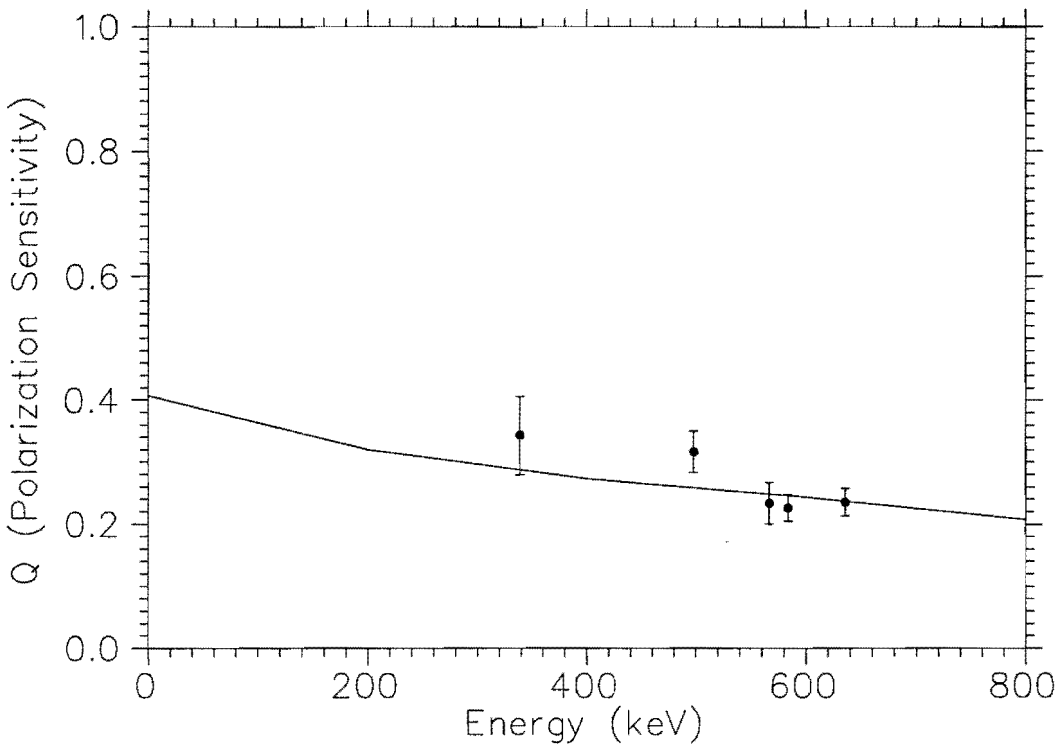

Figure 4.9: *A plot of the polarisation sensitivity of the Clover detector as a function of γ-ray energy. Data points have been fitted with the Klein-Nishina formula (solid line).*

reaction at a beam energy of 150 MeV. The experiment was done at the NAC in 1998 to create Ta nuclei and to study their excited states. Spectra were gated on Ta X-rays in order to enhance Ta transitions and have been used to determine the multipolarity of its γ-rays and to measure the sign of their polarisation.
The main objective of this analysis was to do a viability study of using the NAC Clover detectors as Compton polarimeters and to test if the technique we are developing works and also to apply the technique to another nucleus (^{165}Ta) by measuring the polarisation of its γ-rays associated with the decay of its high spin states.

4.2.1 Discussion

Figure 4.10 shows gated, background subtracted and efficiency corrected add-back spectra. In the upper part the spectrum of events scattered vertically with respect to the beam axis is plotted. The middle part shows the spectrum of events scattered horizontally with respect to the same axis. Most important is the spectrum plotted in the lower part which is a difference between the two spectra mentioned above. ^{165}Ta transitions can be identified in the last spectrum. Between 211 keV to 376 keV lie γ-lines mainly corresponding to magnetic transitions with

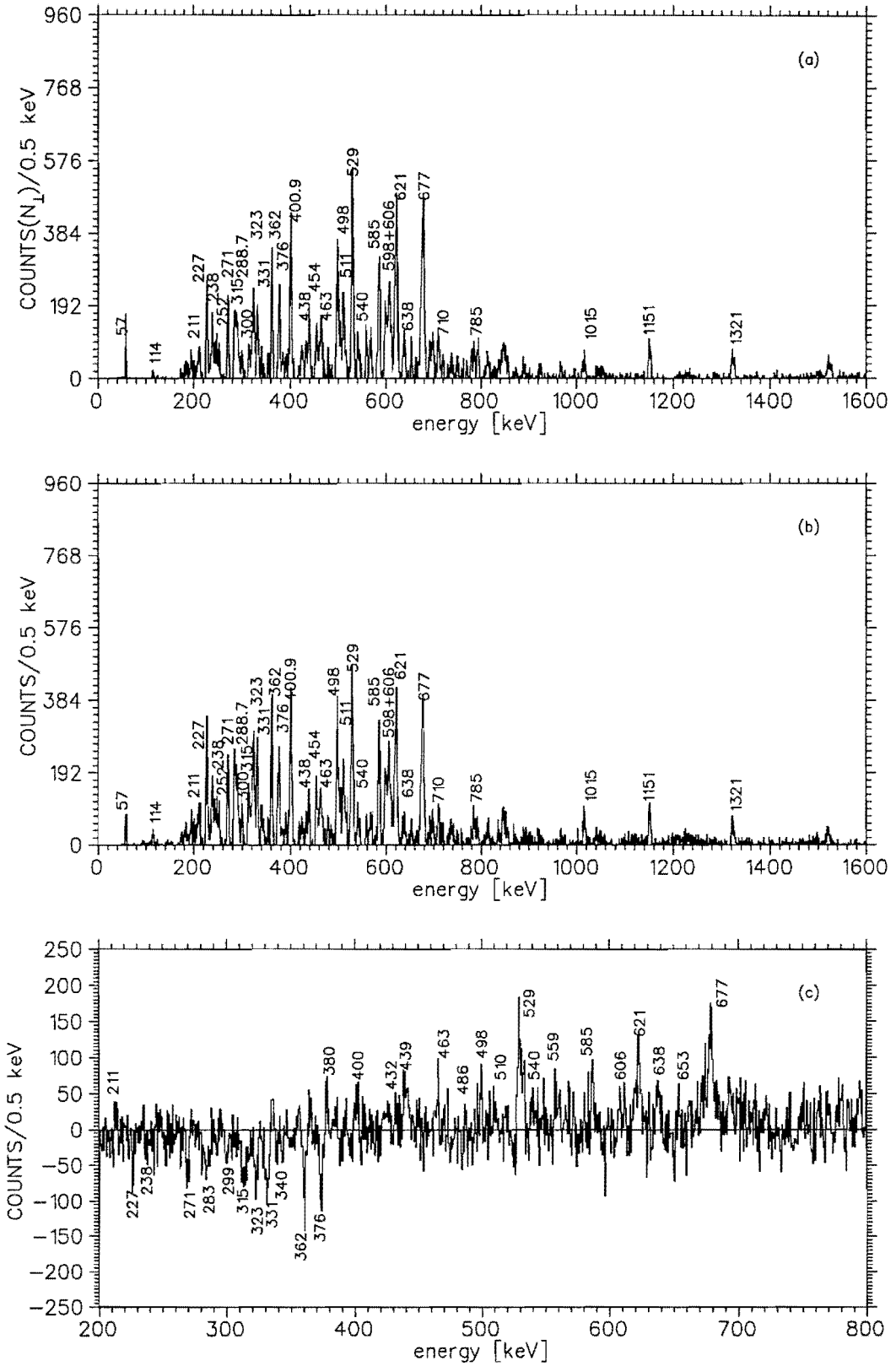

Figure 4.10: *a) and b) : The gated and background subtracted total projection spectra of the vertically and horizontally scattered events, respectively. c) : Difference $N_{\perp} - aN_{||}$spectrum corrected for efficiency, showing which ^{165}Ta γ-lines are polarised.*

$N_\perp$	$N_\parallel$	Energy(keV)	A($\frac{N_\perp - aN_\parallel}{N_\perp + aN_\parallel}$)
2066 ± 45	2512 ± 50	227	-0.0719 ± 0.0109
1689 ± 41	2060 ± 45	271	-0.0735 ± 0.0121
2518 ± 50	3076 ± 55	362	-0.0742 ± 0.0099
2127 ± 46	2516 ± 50	376	-0.0582 ± 0.0102
5521 ± 74	4715 ± 69	529	0.1417 ± 0.0131
3366 ± 58	2916 ± 54	585	0.0971 ± 0.0171
5832 ± 76	5097 ± 71	621	0.0927 ± 0.0131
6420 ± 80	4939 ± 70	677	0.1555 ± 0.0112

Table 4.4: *Anisotropy measurements for the ^{165}Ta nucleus obtained from the difference $N_\perp - aN_\parallel$ between the intensity of events scattered vertically($N_\perp$) and that of events scattered horizontally($N_\parallel$). All these transitions except for the 376 keV γ-line appear on the ^{165}Ta level scheme.*

their counts being negative. Between 380 keV to 677 keV lie γ-lines mainly corresponding to electric transitions with positive counts. The 362 keV and the 376 keV lines appear as strong magnetic transitions while the 529 keV and the 677 keV appear as strong electric transitions.

The intensity of eight ^{165}Ta transitions in the vertical and horizontal spectra was determined using a Radware fitting program, GF2, and their anisotropy calculated as shown in Table 4.4 above, using equation 3.7. Figure 4.11 confirms our results discussed above. The 227, 271, 362 and 376 keV lines appear

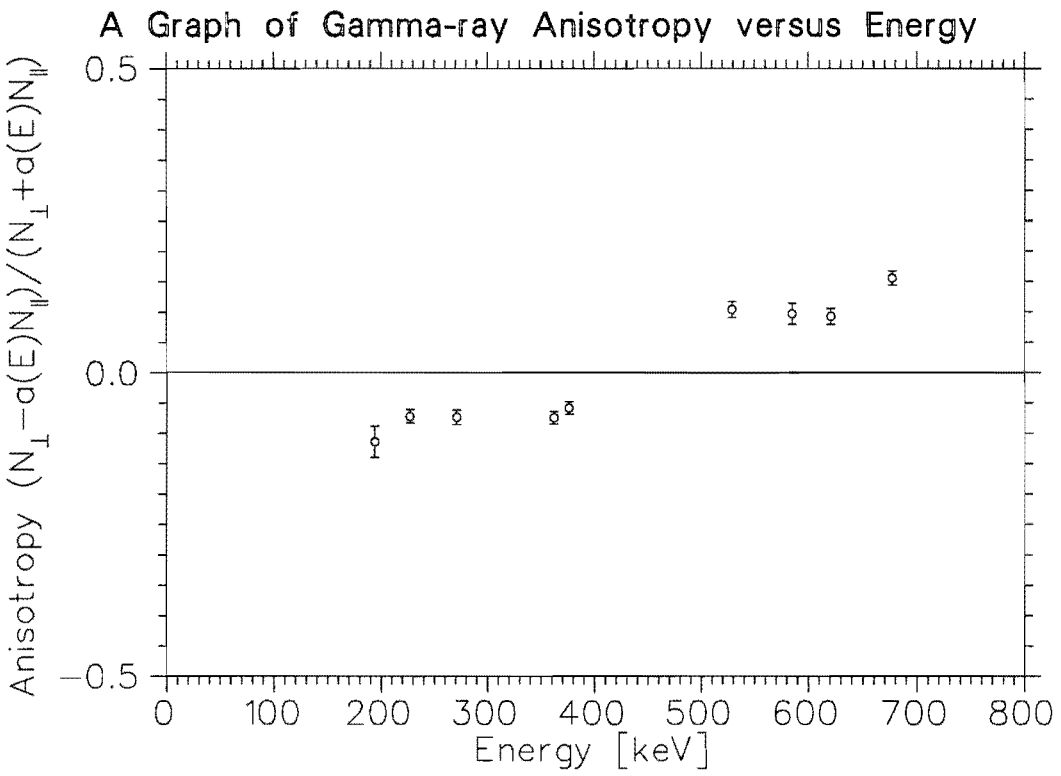

Figure 4.11: *A plot of experimental anisotropy against γ-ray energy showing polarised ^{165}Ta γ-rays and the sign of their polarisation.*

as negative and correspond to the magnetic transitions and the 529, 585, 621 and the 677 keV γ-lines appear as positive and correspond to the electric transitions.

A level scheme of ^{165}Ta is shown in Figure 4.12 [Rou00]. Some of the γ-transitions we have measured are magnetic linking transitions between two bands. Our measurements confirm part of this level scheme and assignments of parity to nuclear spins of selected γ-transitions. The 227 keV γ-line, for example, results from a magnetic dipole and thus there is no change in parity in the decay from the 13/2 to the 11/2 nuclear state.
The same is true for all the other magnetic dipoles and the electric quadrupoles as shown in the level scheme. If you know the parity of the state a nucleus decays from and the radiation character, you can deduce the parity of the state it decays to.

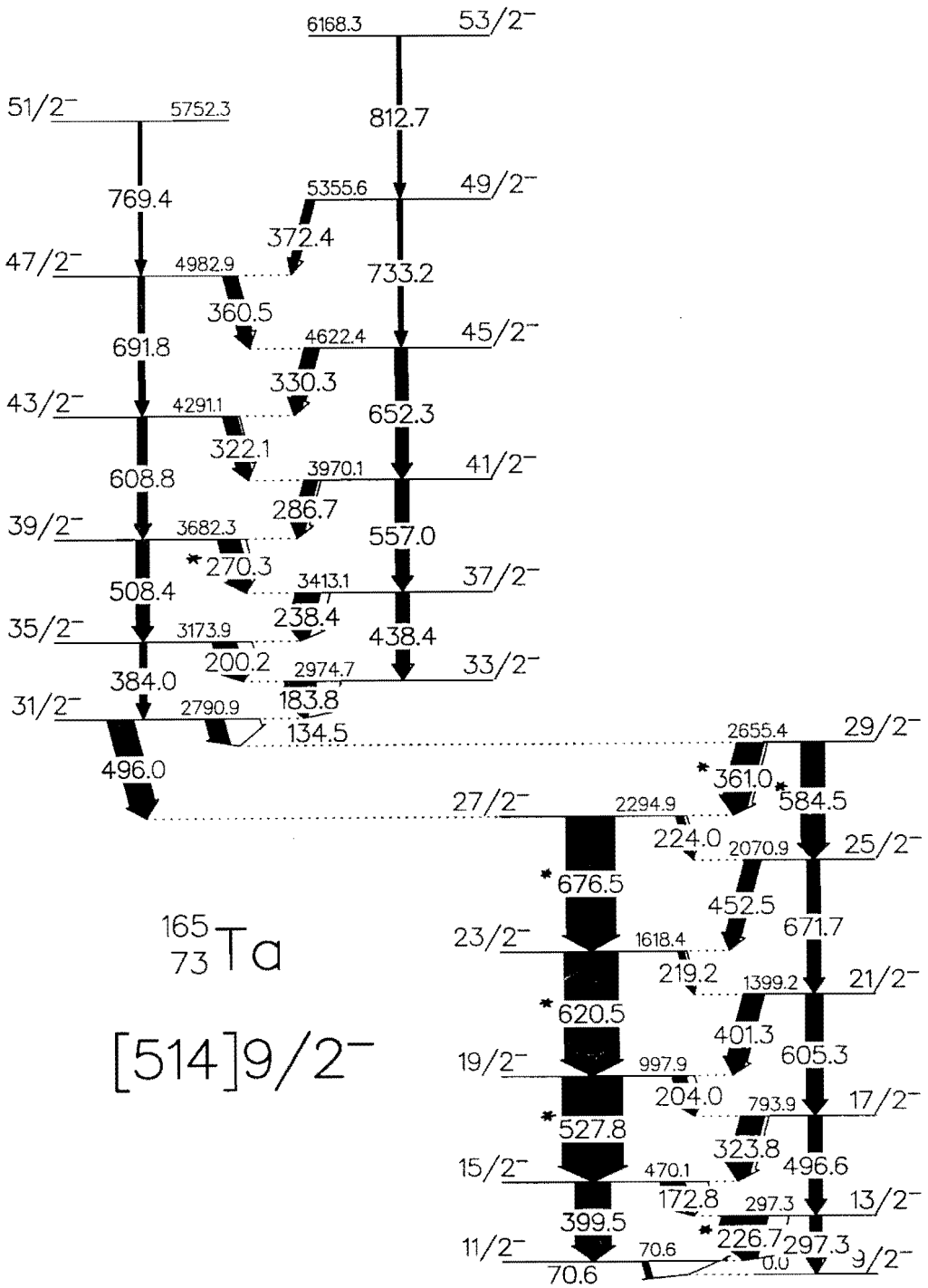

Figure 4.12: *A level scheme diagram of* ^{165}*Ta. The transitions marked with an asterisk have been confirmed through polarisation measurements.*

Chapter 5

CONCLUSION

The development of the HPGe Clover detectors and their use in γ-array spectrometers like EUROGAM-II, EUROBALL and AFRODITE have brought about many advantages with regard to detection and measurement of radiation in nuclear physics [Bea96].

These detectors have high efficiency(ϵ) for detection of γ-rays (the photopeak efficiency for each Clover crystal ϵ, is about 21% measured in singles relative to a 7.62cm x 7.62cm NaI detector at 25cm from the source [Jon95]). The AFRODITE Clover detectors have been geometrically calibrated for their sensitivity to linear polarisation and have been used as Compton polarimeters.

The asymmetry associated with the geometry of the polarimeter, a, has been measured using unpolarised radiation emitted by a

radioactive ^{152}Eu source. The polarimeter has been calibrated using well known $E2$ ^{164}Hf transitions from the ^{142}Nd(^{27}Al, 4np) reaction at a beam energy of 150 MeV. The experiment was done using the AFRODITE detector array at NAC in 1998.

The angular distributions of γ-rays have been measured at different angles which are 45° , 135° and 90° with respect to the beam direction. The angular distribution coefficients have been extracted from equation 2.2 in Chapter Two, and the linear polarisation of seven ^{164}Hf γ-lines has been measured at 90°. Using calculated values of polarisation and the measured anisotropy of γ-transitions, the polarisation sensitivity, Q, has been calculated and found to be 0.34 ± 0.06 at 339.0 keV and 0.24 ± 0.02 at 635 keV. The polarisation sensitivity showed a decrease with increasing energy as expected.

The polarimeter has been applied to determine the multipolarity of ^{165}Ta γ-rays. The character of, among others, eight γ-lines has been determined and four γ-lines which are the 227 keV, 271 keV, 376 keV and 362 keV have been found to be consistent with transitions of magnetic nature (appearing with negative anisotropy) and the other four which are the 529 keV, 585 keV, 621 keV, and 677 keV to the electric transitions (appearing with positive anisotropy).

Figure 4.9 shows a plot of the polarisation sensitivity against the γ-ray energy. It can be seen that some of the data points deviate from the fitted solid line. The point at 339 keV is the most notable in this case and appears with big error bars than those of the other points. The solid line is a fit based on the Klein-Nishina expression. This deviation could be due to systematic errors associated with the peak fitting procedure. Fitting the peaks even more carefully and precisely in future may help improve the technique as that may result in the construction of more precise angular distributions. Also, by doing a software cut on the scattering angle, θ, of a γ-ray, the background due to events that lie outside the physical limits of $\cos\theta$ may be reduced [But72], and hence the polarisation sensitivity of the detectors be improved. A conclusion could still be made though, judging from the results presented in this work, that the technique we have developed at NAC to measure polarisation of γ-rays works.

Appendix A

NUCLEAR ORIENTATION

A.1 Definitions: Polarisation, Orientation, Alignment

Particles emitted from a radioactive source in a field free region are distributed isotropically in space. Isotropic emission results if directions of **I** (spin) and μ_I (magnetic moment) are randomly distributed.

If a certain axis of quantization, Oz, is defined by a vanishingly small magnetic field, then for the whole assembly of nuclei the magnetic substates are equally populated, i.e. with equal number of nuclei pointing in all directions. We say a system is unoriented if the probability P(m) of the occurrence of any particular value m($\hbar$) (a component of the angular momentum) is independent of m. If $P(m)$ depends on m then we say a

system is oriented. If more spins point in one direction (+Oz) than in the opposite direction (-Oz), $P(m) \neq P(-m)$ and the system is said to be polarised. If $P(m)$ depends on m^2 so that $P(m) = P(-m)$ then we say the system is aligned, i.e. the system has equal numbers of nuclei pointing in opposite directions. This system is not polarized but is oriented with respect to the Oz axis. The polarisation P, may be defined as

$$P = \frac{1}{I}\sum mP(m) \tag{A.1}$$

The summation is over all possible magnetic substates. A system of nuclei with spin $\frac{1}{2}$, of which N_1 are pointing 'up' $(m = +\frac{1}{2})$ and N_2 are pointing 'down' $(m = -\frac{1}{2})$ will have,

$$P(\frac{1}{2}) = \frac{N_1}{N_1 + N_2}, \tag{A.2}$$

and

$$P(-\frac{1}{2}) = \frac{N_2}{N_1 + N_2} \tag{A.3}$$

such that

$$P = \frac{N_1 - N_2}{N_1 + N_2}, \tag{A.4}$$

and this gives the excess of spins pointing in one direction provided

$$N_1 \neq N_2$$

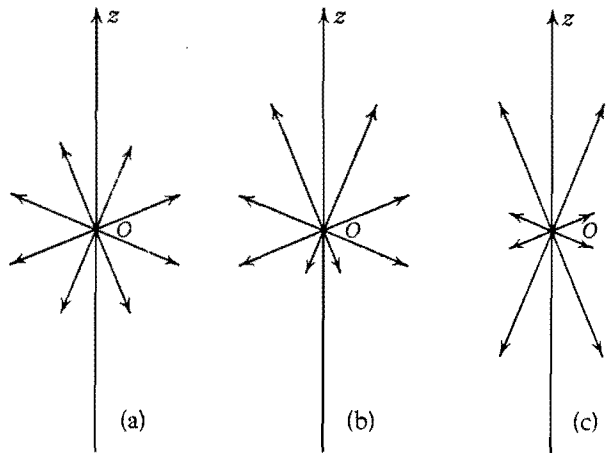

Figure A.1: *A diagram showing a representation of nuclear magnetic substates with Oz being the quantization axis. The lengths and direction of arrows represent the number of nuclei with spins pointing in the same direction. a) Unoriented system as in the case of a radio-active source. b) An oriented system (polarized). c) An oriented system (aligned).*

For $N_1 = N_2$, we have alignment, e.g. for spin 1, nuclei in the substate $m = 0$ form an aligned system. As can be seen above, P is normalized to 1 or -1 [Bur71].

A.1.1 Oriented Nuclear Systems

A.1.1.1 Angular distribution

Measurements of angular distributions of radiation from oriented nuclei is the most usual method of detecting nuclear orientation. The semi-classical theory of radiation indicates that the radiation of multipolarity (L,M) emitted in a transition between nuclear states of spin $(I_i m_i)$ and $(I_f m_f)$ has a definite angular distribution $F_L^M(\theta)$ with respect to the axis of quantization. The selection rules relate the quantum numbers in the form:

$$I_i + I_f \geq L \geq \mid I_i - I_f \mid$$

$$m_i - m_f = M \tag{A.5}$$

where

$$\mid M \mid \leq L$$

Figure A.2 shows a γ-transition between two nuclear states with spins I_i and I_f and their components m_i and m_f, respectively. The figure is taken from [Bur71]. Probably there is an error in

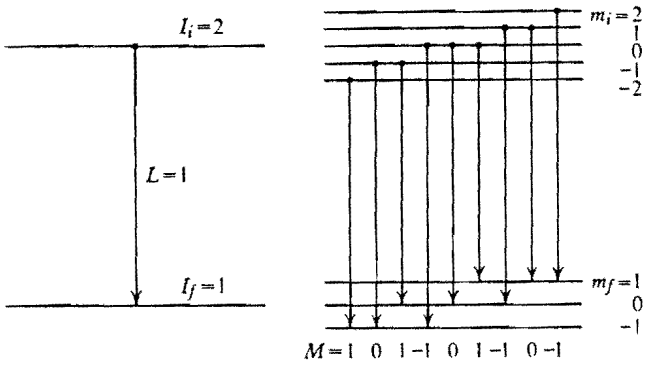

Figure A.2: *This diagram shows a γ-transition of multipole order 1 between two nuclear levels, I_i and I_f.*

the figure as equation A.5 does not agree with the values of M given in the figure.

The angular distribution arising from a given substate m_i of the initial level is given by

$$W(\theta) = \sum_{M} < I_i I_f m_i m_f \mid LM >^2 F_L^M(\theta) \qquad \text{(A.6)}$$

[Bur71] where the probability of the vectors I_i, I_f combining to give a vector L, with particular magnetic quantum numbers, is given by vector addition coefficients. If the initial substate has a probability P(m_i), which depends on m_i, the total angular distribution is

$$W(\theta) = \sum_{M,m_i} P(m_i) < I_i I_f m_i m_f \mid LM >^2 F_L^M(\theta) \qquad \text{(A.7)}$$

This should be a constant if $P(m_i)$ is independent of m_i, i.e. if the initial levels are equally populated. If, for example, $I_i = 1$, $I_f = 0$, $L = 1$(dipole radiation) we have,

$$F_1^0 \propto \sin^2\theta \qquad F_1^{\pm 1} \propto \frac{1+\cos^2\theta}{2} \tag{A.8}$$

and the vector addition coefficients are

$$< 010 \pm 1 \mid 1 \pm 1 >= 1 \qquad < 0100 \mid 10 >= 1 \tag{A.9}$$

such that

$$W(\theta) = \sin^2\theta + 2.\frac{1}{2}(1+\cos^2\theta) \tag{A.10}$$

$$= \text{constant}$$

as expected [Bur71].

If the population of the substates of the initial level are unequal, then the resulting angular distribution is in general anisotropic.

A.1.2 Angular Correlation Of Successive Radiation

Another method of obtaining nuclear orientation is called γ-γ correlation This method can be applied in situations whereby an excited nucleus decays by emitting a cascade of two or more γ-rays. From Figure A.3 I_2 represents the excited state, I_1 the intermediate state and I_0 the ground state of the transition. If

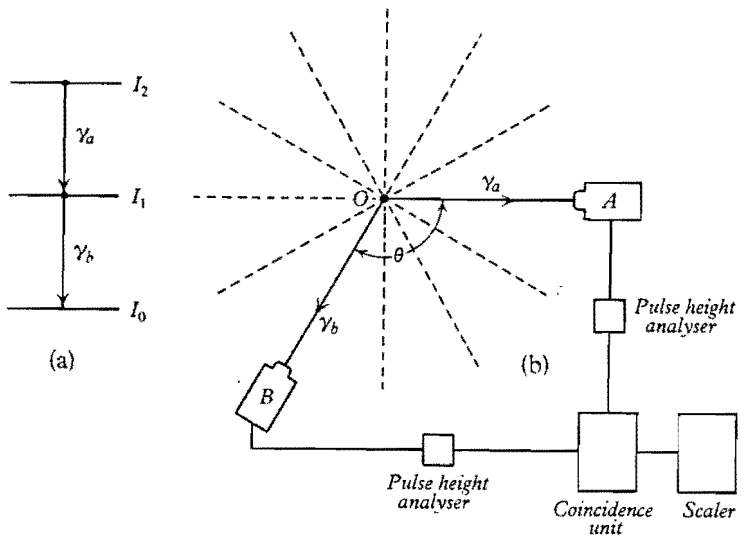

Figure A.3: *Angular correlation of successive radiations from a radioactive nucleus at O. a) Decay scheme. b) Experimental arrangement of counters and coincidence unit. Figure and caption taken from [Bur71].*

a radiation γ_a is observed in a particular direction which defines the axis of quantization, then a set of nuclei in state I_1 after the transition of γ_a will be picked out with an anisotropic distribution of spin directions i.e. the nuclear spins in the intermediate state will be aligned perpendicular to the direction of γ_a. If this distribution of spins persists until γ_b is observed in coincidence with γ_a then an angular distribution of the form

$$W(\theta) = a_0 + a_2 \cos^2\theta + a_4 \cos^4\theta + ... + a_{2L} \cos^{2L}\theta \qquad \text{(A.11)}$$

is obtained.

Appendix B

THE AFRODITE DETECTOR ARRAY

Pictures of the AFRODITE γ-detector array which is being used at NAC (National Accelerator Centre) for high-spin γ-ray spectroscopy are shown below. The performance and characteristics of the array have been discussed in Chapter 3 of this report. The figures-of-merit of the AFRODITE γ-detector array are discussed in detail in [NAC98]. A diagram of the AFRODITE detector array with two of its CLOVER detectors and a LEPS is shown in Figure 3.1 in Chapter 3.

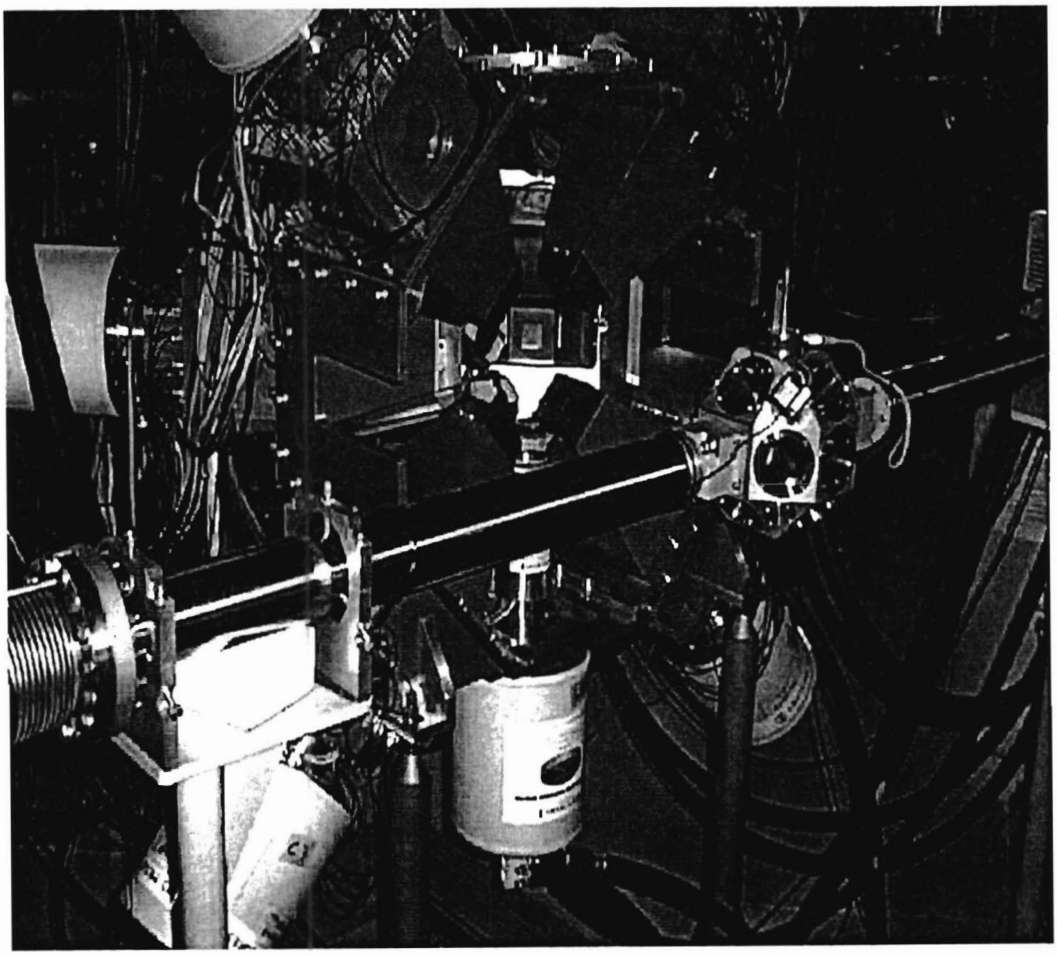

Figure B.1: *Photograph of the inside of the γ-detector array AFRODITE. A beam line connected to the target chamber can be clearly seen.*

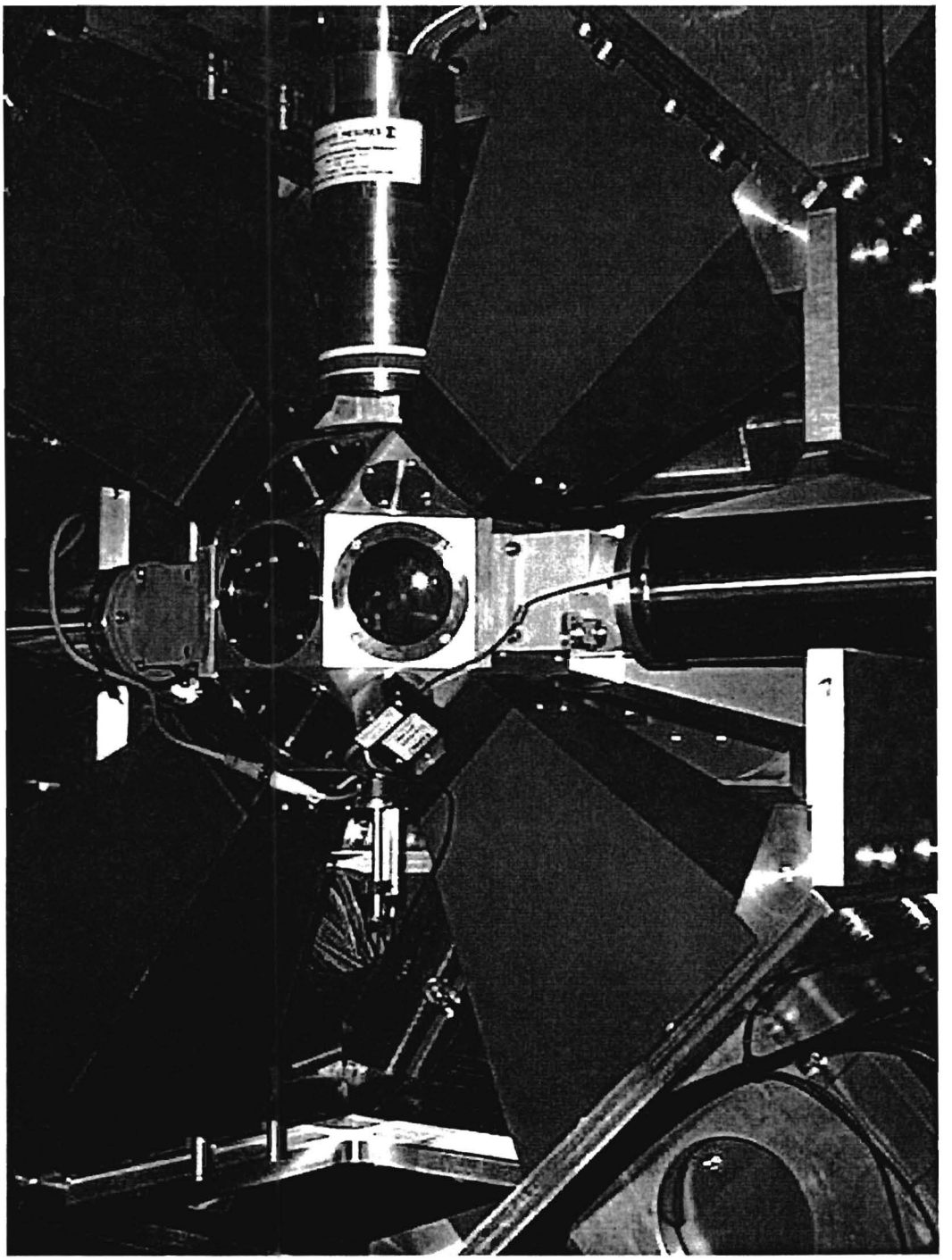

Figure B.2: *Photograph of the γ-detector array showing the target chamber where a target and a radio-active source is placed during in-beam and out-of-beam experiments, respectively.*

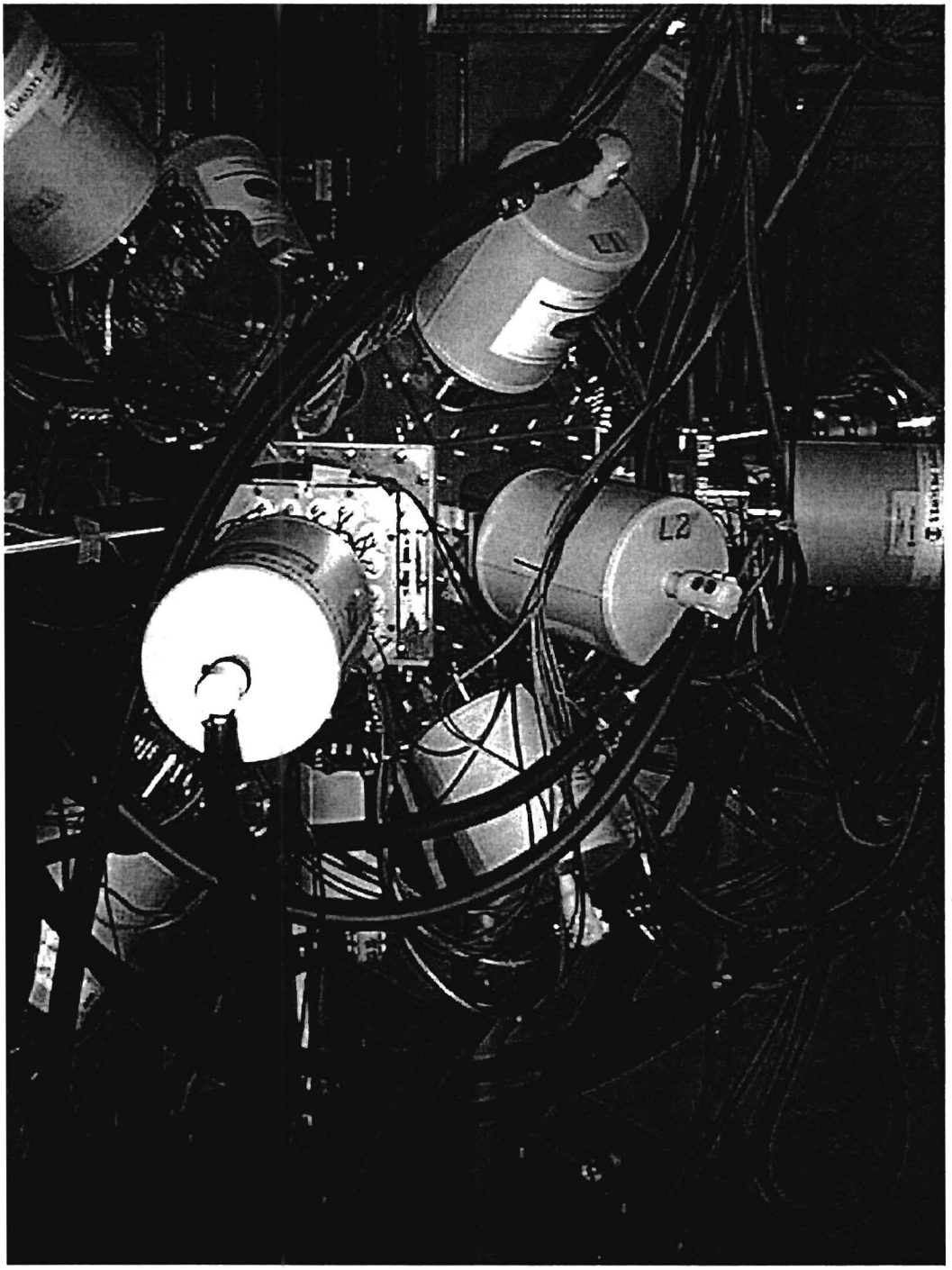

Figure B.3: *Photograph of the outside of the γ-detector array AFRODITE.*

References

[Bas79] R. Bass, J. Idzko, H. Pelz, K. Stelzer, Th. Weber and R. Weniger, Nucl. Instrum. Methods. **163**, 377-387 (1979).

[Bea96] C. W. Beausang and J. Simpson, Report, *Large Arrays of Escape Suppressed Spectrometers for Nuclear Structure Experiments*, (Oliver Lodge Laboratory, The University of Liverpool, L69 3BX, UK, 1996).

[Blu87] K. P. Blume, H. Hübel, M. Murzel, J. Recht, K. Theine, H. Kluge, A. Kuhnert, K. H. Maier, A. Maj, M. Guttormsen, and A. P. De Lima, Nucl. Phys. **A464**, 445-458 (1987).

[Bro69] C. Broude, O. Häusser, H. Malm, J. F. Sharpey-Schafer and T. K. Alexander, Nucl. Instrum. Methods **69**, 29–34 (1969).

[Bur95] W. E. Burcham and M. Jobes, *Nuclear and Particle Physics*, (Longman, Essex, 1995), pp. 184–204.

[Bur71] W. E. Burcham, *Nuclear Physics, an introduction*, (Birmingham, 1971)

[But72] P. A. Butler, P. E. Carr, L. L. Gadeken, A. N. James, P. J. Nolan, J. P. Sharpey-Schafer, P. J. Twin and D. A. Viggars, Nucl. Instrum. Methods **108**, 497–502 (1972).

[Duc99] G. Dûchene, F. A. Beck, P. J. Twin, G. de France, D. Curien, L. Han, C. W. Beausang, M. A. Bentley, P. J. Nolan and J. Simpson, Nucl. Instrum. Methods **A432**, 90–110 (1999).

[Fag59] L. W. Fagg and S. S. Hanna, Rev. Mod. Phy. **31**, 711-757 (1959).

[Gue99] E. Gueorguieva, PhD. Thesis, University of Sophia, Bulgaria, 1999.

[Her99] R. D. Herzberg et al., Phys. Rev **C60**, No. 051307(1999).

[Hol79] A. Holm, IEEE Transactions on Nuc. Sc., **NS26**, 4569–4571, August 1979.

[Jon95] P. M. Jones, L. Wei, F. A. Beck, P. A. Butler, T. Byrski, G. Duchene, G. de France, F. Hannachi, G. D. Jones and B. Kharraja, Nucl. Instrum. Methods **A362**, 556–560 (1995).

[Jos97] P. K. Joshi, H. C. Jain, A. S. Medhi, S. Chattopadhyay, S. Bhattacharya and A. Goswami, Nucl. Instrum. Methods. **A399**, 51–56 (1997).

[Lie95] R. M. Lieder, Report, *Experimental Techniques in Nuclear Physics*, 9–11 (1995) Institut fur Kernphysik, Forschungszentrum Julich, D-52425 Julich.

[Lis78] C. J. Lister, A. M. Al-Naser, A. H. Behbehani, L. L. Green, P. J. Nolan and J. F. Sharpey-Schafer Phys. G: Nucl. Phys., **4**, 907–910, (1978).

[Lju72] A. Ljubicic and B. A. Logan, Nucl. Instrum. Methods. **99**, 269(1972).

[Met50] F. Metzer and M. Deutsch, Phys. Rev., **78**, 551–556, (1950).

[NAC98] R. T. Newman, J.J. Lawrie, B. R. S. Babu, M. S. Fetea, S. V. Förtsch, S. Naguleswaran, J. V. Pilcher, D. A. Raave, C. Rigollet, J. F. Sharpey-

Schafer, C. J. Stevens, F. D. Smit, G. F. Steyn, C. V. Wikner, D. G. Aschman, R. Beetge, R. W. Fearick, G. K. Mabala, S. Murray, D. G. Roux, W. Whittaker and N. J. Ncapayi, NAC Internal Report, NAC/IR/98-01, (National Accelerator Centre, Faure, 1998), pp. 28–29.

[Rad88] D. C. Radford, peak-fitting computer program *GF2*, Physics Division, Oak Ridge National Laboratory, April 1988.

[Rou00] D. Roux et al., *Signature-splitting and quasiparticle alignment in the yrast band of* ^{165}Ta, submitted to Phys. Rev. C (not yet published)

[Sar95] R. A. Sareen, PhD. Thesis, University of Manchester, Manchester, 1995.

[Sch98] G. J. Schmid, A. O. Macchiavelli, S. J. Asztalos, R. M. Clark, M. A. Deleplanque, R. M. Diamond, P. Fallon, R. Kruecken, I. Y. Lee, R. W. MacLeod, F. S. Stephens and K. Vetter, Nucl. Instrum. Methods **A417**, 95–110 (1998).

[Slt94] B. Schlitt, U. Maier, H. Friedrichs, S. Albers, I. Bauske, P. von Brentano, R. D. Heil, R. D. Herzberg,

U. Kneissl, J. Margraf, H. H. Pitz, C. Wesselborg, Nucl. Instrum. Methods **A337**, 416–426 (1994).

[Tar68] P. Tarais, Nucl. Instr. Meth. **61**, 269(1968).

[Twi86] P. J. Twin, Phys. Rev. Lett. **57**, 811 (1986).

[Twi72] P. J. Twin, Nucl. Instrum. Methods **103**, 613–616 (1972).

[Urb87] W. Urban, W. Gast, G. Hebbinghaus, H. M. Jager, A. Kramer-Flecken, R. M. Lieder and M. Thoms, Annual Report, 1987, (Kernforschungsanlage Jűlich GmgH, Institut fur Kernphysik).

[Wer95] A. von der Werth, F. Becker, J. Eberth, S. Freund, U. Hermkens, T. Mylaeus, S. Skoda, H. G. Thomas and W. Teichert, Nucl. Instrum. Methods **A357**, 458–466 (1995).

UNIVERSITY OF CAPE TOWN

Office of the Dean
Faculty of Science
P D Hahn Building, University of Cape Town
7701, Rondebosch, South Africa
Dean: Professor B D Reddy
Tel: +27 21 650 2711
Fax: +27 21 650 2710
E-mail: bdr@psipsy.uct.ac.za

16 November 2000

Prof T Hecht
HOD: Icthyology & Fisheries Science
Rhodes University
Grahamstown

Tel: 27 0 46 603 8415
Fax: 27 0 46 622 4827

Dear Prof Hecht

I shall be most grateful if you would be prepared to act as external examiner for an MSc dissertation that will be submitted to this University.

CANDIDATE'S NAME:	**MR I MATTHEWS**
DEPARTMENT:	**ZOOLOGY**
DISSERTATION TITLE:	**ASPECTS OF THE SETTLEMENT PHASE OF THE MASS CULTURE OF THE SOUTH AFRICAN ABALONE HALIOTIS MIDAE LINN**
HONORARIUM:	**R500**

If you should accept, the dissertation will be sent to you as soon as it is submitted to this office.

Please reply as soon as possible, by return FAX (+27 21 650 2710), completing the section below, informing me whether or not you are able to accept this invitation.

Yours sincerely

Signature Removed

Professor B D Reddy
Dean, Faculty of Science

I ACCEPT/~~DO NOT ACCEPT~~ THE INVITATION TO ACT AS EXTERNAL EXAMINER FOR THE ABOVE STUDENT

I CONFIRM THAT THE PHYSICAL ADDRESS DETAILS ABOVE FOR COURIER DELIVERY ARE CORRECT. ✓ Please tick

Signature Removed DATE 16/11/00